

PLANETARY NEBULAE AS STANDARD CANDLES. II. THE CALIBRATION IN M31 AND ITS COMPANIONS

ROBIN CIARDULLO AND GEORGE H. JACOBY

Kitt Peak National Observatory, National Optical Astronomy Observatories¹

HOLLAND C. FORD²

University of Michigan and Space Telescope Science Institute

AND

JAMES D. NEILL

Space Telescope Science Institute

Received 1988 July 13; accepted September 13

ABSTRACT

We present the results of a planetary nebula survey of M31's bulge performed with the Kitt Peak No. 1 0.9 m telescope and on-band off-band $\lambda 5007$ filters. We detected a total of 429 planetary nebulae (PNs), of which 104 are members of a statistically complete and homogeneous sample covering the top 2.5 mag of the planetary nebula luminosity function (PNLF). We show that the PNLF is clearly not a power law, but instead has a sharp turnover beginning at an equivalent V -magnitude of $M_{5007} \sim -3.8$ and going to zero at $M_{5007}^* = -4.48$. This behavior is most easily explained as arising from a sharp cutoff in the upper mass limit of PN central stars in combination with extremely rapid evolutionary time scales for more massive candidate progenitors. In addition, our analysis of the PN spatial distribution shows that the density of planetary nebulae per unit luminosity is approximately the same in M31's bulge and disk, and the implied stellar death rate is in good agreement with theoretical estimates.

Both the distinctive shape of the PNLF and the invariance of the luminosity-specific PN number density demonstrate that bright planetary nebulae make excellent standard candles. We therefore lay the foundation for extragalactic distance estimates by deriving two maximum-likelihood equations: one which takes advantage of theoretical constraints on the luminosity-specific PN density, and one which is solely dependent on the shape of the PNLF. We explore this technique using new CCD [O III] $\lambda 5007$ photometry of planetaries observed in the M31 companion galaxies M32, NGC 205, and NGC 185.

Subject headings: galaxies individual (M31) — galaxies: stellar content — luminosity function — nebulae: planetary

I. INTRODUCTION

Baade (1955) was the first person to identify planetary nebulae (PNs) in M31. Using the Palomar 5 m telescope with photographic plates and a 1500 Å broad-band filter, Baade detected the [O III] $\lambda 5007$ emission from five planetaries in a disk field 96' southwest of M31's center. The photographic magnitudes of these objects were all between $21.7 < m_{pg} < 22.2$. By using an image tube on the Shane 3 m telescope and restricting the filter bandpass to 23 Å, Ford and Jacoby (1978a) observed planetaries several magnitudes fainter than this, and, in a survey of M31's bulge, found 311 PN candidates, the brightest of which has $m_V = 20.6$. Further large-telescope surveys have cataloged planetaries in M32 (Ford, Jenner, and Epps 1973; Ford and Jenner 1975; Ford 1983), NGC 205 (Ford, Jenner, and Epps 1973; Ford 1978), NGC 185 (Ford, Jenner, and Epps 1973; Ford, Jacoby, and Jenner 1977), and NGC 147 (Ford, Jacoby, and Jenner 1977).

Although PNs were recognized as potential extragalactic standard candles in the early 1960s (Hodge 1966, p. 130) no attempt was made to use these objects until Ford and Jenner (1978) noted that the absolute [O III] fluxes of the brightest

PNs in the Local Group were comparable, and used this fact to derive a distance to M81. Jacoby and Lesser (1981) later utilized this invariance to estimate the distance to the nearby dwarf galaxies IC 10, Leo A, Sextans A, Pegasus, and WLM, and Lawrie and Graham (1983) derived a distance to NGC 300 based on 11 bright PNs in that galaxy. Until now, however, no rigorous or systematic investigation of PN-based distance estimates has been performed.

It is an observed fact that the absolute [O III] $\lambda 5007$ luminosities of the brightest planetary nebulae in the LMC, the SMC, M31, M32, NGC 185, and NGC 147 are all approximately the same. This suggests that a natural limit exists for the luminosity of a planetary. If this is true, then PNs are one of the best standard candles. Not only are these objects bright, relatively easy to detect, and located in regions with little interstellar extinction, but the number of planetaries occurring in a galaxy is a direct measure of the stellar death rate in the underlying population. Since the luminosity-specific stellar death rate is extremely insensitive to details such as the population's age or initial mass function (Renzini and Buzzoni 1986), any distance estimate derived from PNs is immediately verifiable via the implied number of stellar deaths.

This is the second in a series of papers concerned with obtaining distances using the [O III] $\lambda 5007$ flux from planetaries in galaxies beyond the Local Group. In Paper I, Jacoby (1989) discussed the reasons why one can expect an upper limit

¹ The National Optical Astronomy Observatories are operated by the Association of Universities for Research in Astronomy, Inc., under contract with the National Science Foundation.

² Visiting Astronomer, Kitt Peak National Observatory.

to the [O III] flux from planetaries and presented theoretical planetary nebula luminosity functions (PNLFs). In this paper, we use new CCD photometry of 429 bulge and inner disk planetaries in M31 to create an empirical PNLf and develop the procedures required to compute extragalactic distances based on maximum-likelihood statistics. We also apply these equations to new CCD observations of PNs in M32, NGC 205, and NGC 185 in order to demonstrate the technique and explore the possible errors. In subsequent papers, we will compare the PNLf's of several early-type galaxies in the NGC 3379 group, and obtain distances to galaxies such as M81, NGC 5128, NGC 3115, and NGC 5866. An overview of this program was presented by Ford *et al.* (1988). The preliminary distances given in that paper will be superseded by distances based on the planetary nebula calibration given here.

II. OBSERVATIONS AND REDUCTIONS

An area along M31's major axis extending 30.4 to the northeast and 10.2 to the southwest of the nucleus was surveyed with an RCA CCD camera at the f/7.5 focus of the Kitt Peak No. 1 0.9 m telescope. Observations were taken through two filters: an [O III] filter corrected for the peculiar velocity of M31 (central wavelength, $\lambda_c = 5004 \text{ \AA}$; full width at half-maximum [FWHM] = 27 \AA) and one of three off-band [O III] filters, which were used as a comparison for identification of the emission-line sources. The on-band [O III] exposure times were 1 hr, while the off-band exposures varied depending on the width of the filter. To ensure against the possible misidentification of strong absorption line objects as emission-line sources, the off-band exposure times were chosen to go ~ 0.25 mag deeper than the on-band frames.

The survey region is displayed in Figure 1 (Plate 1). Two frames are centered on M31's nucleus, and another two contain the nucleus in either the southwest or the northeast corner. The remaining nine frames are arranged along the major axis in such a way that each field overlaps the next, thus enabling all the images to be placed on a common astrometric and photometric system. A log of the observations appears in Table 1.

After the CCD frames were debiased and flat-fielded, every [O III] image was blinked against its off-band counterpart to detect stellar objects emitting in the 5007 \AA line of [O III].

Objects that were extended or that appeared in the off-band image were rejected as PN candidates. The finder charts and coordinates of Ford and Jacoby (1978b) and the coordinates of Lawrie and Ford (1982) were then used to identify previously discovered PNs or to assign unique identification numbers to the new objects. The ID numbers of the current survey are a continuation of those of Nolthenius and Ford (1987).

Of the 244 Ford and Jacoby (1978b) PNs included in our survey region, 13 could not be detected and four were observable on continuum frames. Of the 19 additional PNs reported by Lawrie and Ford (1982), four were confirmed with these new observations. Table 2 contains the positions and equivalent V -magnitudes for all the planetaries detected in the present survey. Those candidates of the previous surveys which could not be confirmed with the CCD, or which proved to be continuum sources, are listed in Table 3.

Raw magnitudes for the planetary nebulae and a set of comparison stars were measured using Stetson's DAOPHOT photometry package. Aperture photometry on each object was performed by summing the counts within a 2 pixel ($1''.72$) radius of the star's centroid and subtracting the sky, as determined from an annulus 10–15 pixels from the star. For objects in M31's outer bulge, this straightforward technique yielded acceptable results. However, for planetaries near the nucleus, the uncertainty introduced by the rapidly varying galaxy background was large. Therefore, to reduce the error, those off-band frames containing the nucleus were spatially registered and intensity-scaled to match their corresponding on-band frames. PN aperture photometry was then performed on the [O III] minus off-band difference images. This technique removed the background galaxy but left the emission-line sources intact and significantly reduced the photometric errors in the inner regions.

After determining raw instrumental magnitudes, standard $\lambda 5007$ magnitudes were found using the SUPERPHOT analysis package described by Ciardullo *et al.* (1987). This program enables a set of overlapping CCD fields to be tied onto a common photometric system by solving the least-squares condition required to match the magnitudes of stars in the regions of field overlap. The zero point of the system was then determined by performing large-aperture absolute photometry on the foreground stars of fields 1 and 10, and compar-

TABLE 1
LOG OF M31 PLANETARY NEBULA OBSERVATIONS

FIELD	$\alpha(1975)$	$\delta(1975)$	UT DATE	CCD	EXPOSURE (s)	OFF-BAND FILTER	
						λ_c /FWHM (\AA)	Exposure (s)
1	0 ^h 41 ^m 38 ^s .0	41 ^o 09'31"	1984 Sep 30	RCA 1	3600	5297/104	1200
2	0 41 07.2	41 06 25	1984 Oct 31	RCA 1	3600	5297/104	1200
3	0 41 39.3	41 11 44	1984 Nov 3	RCA 1	3600 ^a	5297/104	1200
4	0 41 23.0	41 08 16	1985 Sep 13	RCA 3	3600	5307/236	450
5	0 41 51.7	41 16 47	1985 Sep 13	RCA 3	3600	5307/236	450
6	0 41 07.4	41 02 13	1985 Sep 14	RCA 3	3600	5307/236	450
7	0 41 04.1	41 01 51	1985 Oct 13	RCA 3	3600	5307/236	450
8	0 41 24.0	41 07 25	1985 Oct 15	RCA 3	3600	5307/236	450
9	0 41 43.7	41 11 17	1986 Oct 5	RCA 3	3600	5279/279	450
10	0 42 05.0	41 14 24	1986 Oct 5	RCA 3	3600	5279/279	450
11	0 42 28.0	41 17 54	1986 Oct 7	RCA 3	3600	5279/279	450
12	0 42 49.8	41 21 14	1986 Oct 7	RCA 3	3600	5279/279	450
13	0 43 12.0	41 24 30	1986 Oct 7	RCA 3	3600	5279/279	450

^a A sum of two 1800 s exposures.

PLATE 1

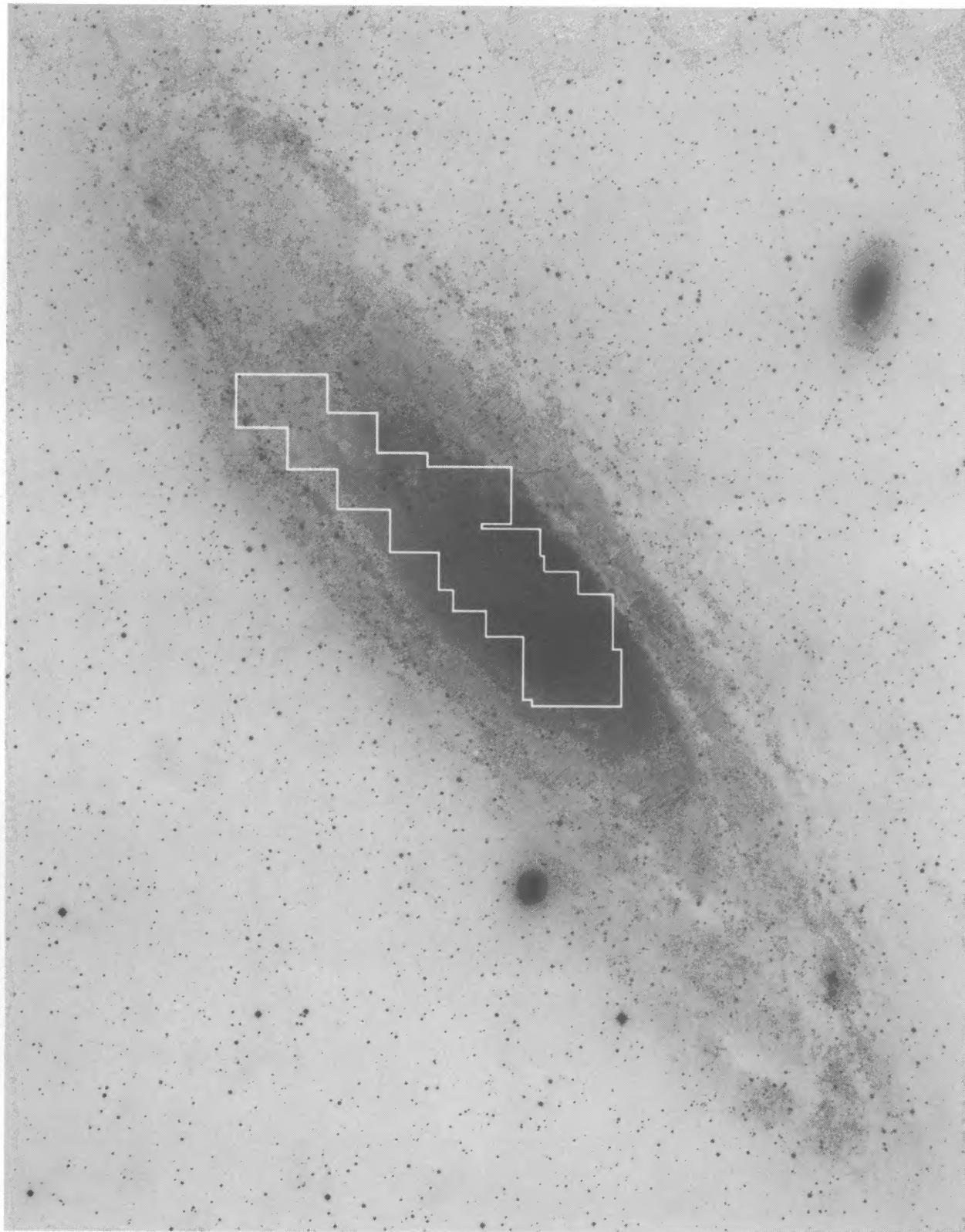


FIG. 1.—Region covered by our M31 PN CCD survey superposed on a Palomar Schmidt plate of M31's central $1'.5$. North is at the top, and east is to the left. The frames extend roughly $30'.4$ northeast and $10'.2$ southwest along the major axis.

CIARDULLO, JACOBY, FORD, AND NEILL (*see* 339, 54)

TABLE 2
M31 PLANETARY NEBULAE

ID	$\alpha(1975)$	$\delta(1975)$	N	m_{5007}	s.e.(m)	Sample	ID	$\alpha(1975)$	$\delta(1975)$	N	m_{5007}	s.e.(m)	Sample
1	0 41 23.91	41 08 28.7	4	20.73	0.02	B	53	0 41 13.02	41 06 33.5	3	20.43	0.00	AB
2	0 41 23.70	41 08 11.8	3	21.40	0.03		54	0 41 14.84	41 06 22.7	3	20.57	0.01	AB
3	0 41 21.46	41 08 13.0	4	21.05	0.03		55	0 41 16.14	41 06 21.9	3	21.39	0.03	AB
5	0 41 20.08	41 07 40.8	3	21.18	0.01	B	56	0 41 18.45	41 05 57.3	2	20.94	0.01	AB
6	0 41 20.87	41 07 36.4	2	22.41	0.04		57	0 41 19.86	41 05 56.8	2	21.08	0.04	AB
7	0 41 21.03	41 07 43.5	3	21.56	0.05	B	58	0 41 21.59	41 06 37.9	3	21.01	0.02	B
8	0 41 21.53	41 07 48.5	3	21.43	0.02		59	0 41 23.78	41 07 03.8	3	21.72	0.04	
9	0 41 22.94	41 07 53.0	3	21.47	0.02		60	0 41 25.26	41 06 52.5	3	21.56	0.03	
10	0 41 24.42	41 07 56.9	4	21.20	0.02		61	0 41 24.46	41 06 08.7	3	20.97	0.02	AB
12	0 41 25.28	41 08 09.0	4	20.75	0.00	B	62	0 41 26.64	41 07 11.6	1	21.10	...	
13	0 41 25.00	41 08 15.8	4	21.48	0.01	B	63	0 41 27.07	41 06 44.1	2	21.67	0.01	
14	0 41 24.66	41 08 42.3	2	22.05	0.07		64	0 41 30.44	41 06 03.3	2	20.73	0.03	
15	0 41 24.16	41 08 49.7	3	21.66	0.04	B	65	0 41 17.15	41 06 04.8	3	22.23	0.01	A
16	0 41 18.65	41 07 59.4	1	21.79	...	B	66	0 41 17.84	41 06 25.7	3	22.13	0.05	
17	0 41 17.49	41 07 36.6	3	20.73	0.00		67	0 41 24.40	41 05 03.7	1	20.78	...	AB
18	0 41 17.48	41 07 23.9	3	20.89	0.02	B	68	0 41 20.08	41 04 50.8	1	21.81	...	AB
20	0 41 20.78	41 07 24.0	3	21.55	0.02	B	69	0 41 14.68	41 03 57.0	2	20.96	0.02	
21	0 41 22.91	41 07 10.8	3	21.18	0.01		70	0 41 16.73	41 06 43.8	3	22.04	0.02	A
23	0 41 26.67	41 08 43.2	3	21.45	0.03	B	71	0 41 15.24	41 06 22.2	3	21.96	0.04	AB
24	0 41 31.09	41 08 15.7	3	21.31	0.03	AB	72	0 41 24.09	41 07 33.5	4	21.68	0.03	
25	0 41 32.33	41 08 11.8	3	21.80	0.01	AB	74	0 41 22.64	41 07 08.3	3	21.70	0.04	B
26	0 41 33.22	41 08 12.2	2	20.98	0.00	AB	75	0 41 29.06	41 07 43.9	3	21.85	0.03	
27	0 41 35.69	41 08 09.1	3	20.85	0.01	AB	76	0 41 32.30	41 07 25.0	3	21.94	0.01	
28	0 41 29.83	41 09 12.2	4	20.64	0.02	AB	77	0 41 32.31	41 07 09.4	2	21.96	0.11	AB
29	0 41 31.24	41 09 21.6	4	21.01	0.01	AB	78	0 41 28.63	41 06 34.9	2	22.01	0.00	
30	0 41 33.15	41 09 08.5	4	20.70	0.01	AB	79	0 41 26.39	41 06 13.5	3	22.17	0.03	A
31	0 41 36.03	41 08 57.5	3	20.49	0.01	AB	80	0 41 35.04	41 09 13.2	4	21.00	0.01	AB
32	0 41 31.06	41 10 04.8	4	20.77	0.02	AB	81	0 41 21.13	41 08 44.6	3	22.73	0.16	
33	0 41 35.45	41 10 35.7	2	21.75	0.02		82	0 41 17.54	41 08 50.6	1	22.95	...	
34	0 42 03.78	41 17 42.0	1	23.58	...		83	0 41 19.10	41 09 36.5	3	22.37	0.05	A
35	0 41 16.02	41 07 21.0	3	21.43	0.02	B	87	0 41 15.80	41 08 40.0	2	21.66	0.07	
36	0 41 15.15	41 07 38.5	3	21.01	0.00	B	91	0 40 58.57	41 08 40.6	1	22.92	...	
37	0 41 14.94	41 08 13.9	3	22.13	0.04	A	92	0 41 00.14	41 07 51.7	1	20.87	...	
38	0 41 15.49	41 08 30.6	3	21.37	0.02	AB	93	0 41 03.38	41 07 30.1	1	20.95	...	AB
39	0 41 14.16	41 08 44.6	2	21.88	0.02	AB	94	0 41 05.05	41 07 21.2	3	21.93	0.01	
40	0 41 13.78	41 08 21.7	3	21.49	0.02	AB	95	0 41 06.10	41 07 16.5	3	21.13	0.01	AB
41	0 41 10.97	41 08 36.7	3	20.63	0.01		97	0 40 59.62	41 05 58.7	1	20.61	...	AB
42	0 41 10.52	41 08 20.0	3	20.43	0.01		98	0 41 07.45	41 05 39.4	2	21.65	0.01	AB
43	0 41 08.77	41 08 12.5	3	21.23	0.02	AB	99	0 41 20.19	41 05 43.7	2	21.97	0.00	AB
44	0 41 09.22	41 08 02.2	3	21.99	0.01	AB	100	0 41 05.32	41 07 54.4	3	21.72	0.03	AB
45	0 41 10.27	41 07 45.9	3	20.60	0.01	AB	101	0 41 04.92	41 06 42.0	2	22.10	0.04	A
46	0 41 05.54	41 08 18.3	3	20.32	0.04	AB	102	0 41 17.27	41 10 18.8	1	22.62	...	
47	0 41 05.53	41 08 06.8	3	20.72	0.01	AB	103	0 41 17.93	41 10 29.3	1	23.02	...	
48	0 41 06.83	41 07 03.7	3	20.31	0.01	AB	105	0 41 18.96	41 10 56.0	1	22.51	...	
49	0 41 04.96	41 06 21.8	3	20.54	0.02	AB	107	0 41 23.17	41 11 05.9	2	22.44	0.07	
50	0 41 07.31	41 05 51.8	2	20.83	0.02	AB	109	0 41 23.17	41 11 44.8	2	22.67	0.11	
51	0 41 11.88	41 06 52.0	3	20.99	0.02	AB	112	0 41 27.37	41 10 28.5	4	22.85	0.13	
52	0 41 12.46	41 06 32.2	2	21.63	0.05	AB	113	0 41 27.53	41 11 55.3	2	22.17	0.07	

ing their $\lambda 5007$ magnitudes to those observed for the spectrophotometric standards of Oke (1974) and Stone (1977). In all, 13 observations of the stars BD +28°4211, BD +40°4032, Feige 25, and EG 247 were used to convert the instrumental PN magnitudes into apparent monochromatic fluxes above the Earth's atmosphere. The scatter in each individual standard star measurement was $\sim 3\%$. The estimated uncertainty in the adopted zero point of the system is less than 1%.

The last step in the reduction consisted of transforming the apparent monochromatic fluxes in the $\lambda 5007$ filter into standard magnitudes. Following the procedure described by Jacoby, Quigley, and Africano (1987), the total [O III] $\lambda 5007$ flux of each planetary was computed using its apparent monochromatic flux and a measurement of the filter transmission

curve. Following Paper I, this flux was then converted into an equivalent V -magnitude using the equation

$$m_{5007} = -2.5 \log F_{5007} - 13.74. \quad (1)$$

These magnitudes are listed in Table 2. For objects with multiple measurements, the standard errors in the magnitudes are also included.

The equatorial positions of the planetary nebulae were calculated by once again taking advantage of the overlap regions in the CCD fields and bootstrapping from known astrometric standards. First, a set of comparison stars was selected, many of which were secondary standards of Ford and Jacoby (1978b) and Ciardullo *et al.* (1987). For each CCD frame containing four or more stars with known positions, an astrometric solution was found and used to compute the coordinates of its

TABLE 2—Continued

ID	$\alpha(1975)$	$\delta(1975)$	N	m_{5007}	s.e.(m)	Sample	ID	$\alpha(1975)$	$\delta(1975)$	N	m_{5007}	s.e.(m)	Sample
114	0 41 25.63	41 12 46.6	2	22.15	0.03		176	0 41 31.94	41 07 15.4	2	23.46	0.29	
116	0 41 32.19	41 13 10.8	2	20.69	0.00	AB	177	0 41 40.09	41 08 37.4	3	22.01	0.02	A
117	0 41 33.90	41 13 50.5	1	21.75	...		178	0 41 47.17	41 07 40.9	1	20.48	...	
120	0 41 33.79	41 09 20.1	4	22.37	0.04	A	179	0 41 41.41	41 09 25.1	4	22.43	0.08	A
121	0 41 33.86	41 10 47.9	1	23.10	...		180	0 41 36.65	41 10 42.3	3	22.49	0.07	A
122	0 41 33.90	41 11 00.5	3	22.26	0.03		181	0 41 18.09	41 05 57.2	2	21.85	0.05	AB
123	0 41 32.45	41 11 41.2	3	22.00	0.03		182	0 41 00.59	41 07 19.4	1	21.73	...	
124	0 41 38.55	41 10 30.2	3	21.44	0.02	AB	183	0 41 02.25	41 06 26.3	1	22.67	...	A
125	0 41 42.90	41 09 25.7	2	21.80	0.04	AB	184	0 41 14.55	41 04 58.3	1	22.95	...	
126	0 41 43.39	41 10 01.4	3	22.30	0.04	A	189	0 41 35.07	41 09 02.5	2	22.69	0.25	
127	0 41 43.69	41 10 16.1	3	22.18	0.07	A	190	0 41 33.01	41 10 02.6	3	22.51	0.13	A
128	0 41 44.30	41 10 25.3	3	21.21	0.02	AB	191	0 41 34.63	41 10 01.9	3	22.85	0.13	
129	0 41 46.73	41 10 31.7	3	21.88	0.01	AB	195	0 41 43.03	41 10 20.4	3	22.58	0.06	A
130	0 41 43.59	41 11 03.5	2	22.01	0.00	A	196	0 41 44.78	41 10 23.9	2	23.09	0.07	
131	0 41 44.98	41 11 09.7	2	20.96	0.01		197	0 41 40.51	41 11 33.4	2	23.59	0.17	
132	0 41 43.07	41 11 16.1	2	22.54	0.00	A	198	0 41 38.87	41 11 52.3	2	22.62	0.08	A
133	0 41 46.47	41 11 48.5	2	21.46	0.00		199	0 41 42.03	41 11 56.0	2	22.54	0.06	
134	0 41 43.81	41 11 51.1	1	21.65	...	AB	200	0 41 40.23	41 12 16.0	1	22.81	...	
135	0 41 37.62	41 08 36.8	3	21.73	0.02		201	0 41 40.65	41 12 28.2	2	22.48	0.13	A
136	0 41 34.91	41 08 46.9	3	22.10	0.02		202	0 41 47.16	41 11 42.5	3	22.75	0.05	
137	0 41 27.85	41 07 14.1	2	22.33	0.09		203	0 41 48.45	41 11 41.4	3	21.77	0.01	AB
139	0 41 20.86	41 05 56.6	2	22.59	0.12	A	204	0 41 50.60	41 12 04.2	2	23.01	0.21	
140	0 41 15.79	41 05 31.7	1	21.34	...	AB	205	0 41 43.83	41 12 07.2	1	22.60	...	A
141	0 41 19.10	41 05 54.7	2	22.24	0.03	A	206	0 41 50.60	41 10 37.2	3	22.31	0.03	
142	0 41 10.63	41 07 45.6	3	21.74	0.03	AB	207	0 41 53.32	41 09 48.6	3	22.38	0.01	A
143	0 41 16.11	41 06 14.8	3	22.91	0.06		208	0 41 57.07	41 09 33.7	3	22.23	0.02	A
144	0 41 13.99	41 03 52.3	2	21.90	0.01	AB	209	0 41 58.51	41 09 39.3	1	21.24	...	
145	0 41 11.62	41 04 54.7	1	22.28	...	A	210	0 41 55.79	41 11 22.8	3	21.64	0.04	
147	0 41 03.72	41 04 18.8	2	21.65	0.02	AB	211	0 41 54.90	41 11 21.0	1	22.42	...	
148	0 41 02.80	41 04 03.9	2	22.40	0.11	A	212	0 41 53.45	41 11 13.7	1	22.47	...	
149	0 41 02.18	41 03 59.0	2	21.37	0.00	AB	213	0 41 55.64	41 11 31.1	3	22.64	0.05	
150	0 41 07.25	41 02 37.2	2	21.28	0.01		214	0 41 54.31	41 11 34.0	2	22.93	0.10	
151	0 41 10.35	41 02 01.9	2	20.92	0.01		216	0 42 04.23	41 12 14.3	1	21.11	...	AB
152	0 41 13.54	41 02 48.6	2	21.74	0.00		217	0 41 55.64	41 13 22.4	3	22.14	0.03	
153	0 41 19.26	41 01 46.1	2	21.71	0.03		218	0 41 51.78	41 13 00.5	2	22.44	0.19	
154	0 41 20.65	41 01 09.7	2	21.01	0.00		219	0 41 50.19	41 13 04.6	2	20.79	0.03	
155	0 41 21.60	41 02 34.0	2	20.50	0.01		220	0 41 42.43	41 13 30.8	2	22.40	0.11	
157	0 41 22.69	41 03 58.7	2	21.36	0.01	AB	221	0 41 37.04	41 13 33.7	1	22.04	...	
159	0 41 17.88	41 05 11.9	2	22.60	0.11	A	222	0 41 31.14	41 11 39.5	3	22.40	0.07	
160	0 41 17.99	41 05 38.3	1	22.90	...		223	0 41 30.50	41 12 06.6	2	23.34	0.06	
163	0 41 25.39	41 05 35.6	2	22.11	0.01		224	0 41 30.31	41 12 10.4	2	22.66	0.11	
164	0 41 27.01	41 05 41.1	1	22.05	...	A	225	0 41 30.38	41 12 50.9	2	23.41	0.14	
165	0 41 25.32	41 06 47.0	3	22.67	0.04		227	0 41 27.15	41 13 58.0	1	23.29	...	
166	0 41 26.76	41 06 29.8	2	22.48	0.16		231	0 41 37.32	41 14 55.7	1	22.56	...	
167	0 41 34.11	41 05 16.5	1	21.11	...		232	0 41 35.12	41 14 53.2	1	21.72	...	
171	0 41 34.64	41 05 56.1	1	22.80	...		233	0 41 35.27	41 16 21.4	1	21.66	...	
172	0 41 38.32	41 06 30.6	2	20.90	0.00		234	0 41 36.05	41 16 58.8	1	21.94	...	
173	0 41 35.73	41 06 39.9	2	22.81	0.00		235	0 41 41.20	41 16 23.1	1	22.87	...	
174	0 41 19.90	41 06 10.3	3	22.36	...	A	237	0 41 50.87	41 16 10.1	2	21.69	0.02	
175	0 41 33.50	41 08 03.6	3	22.13	0.01		239	0 41 50.01	41 17 13.9	1	23.75	...	

remaining comparison stars. The comparison star measurements for all these frames were then combined to yield the astrometric positions of what were now tertiary standards. The procedure was then repeated until an astrometric solution existed for each CCD frame. Finally, the positions of the planetary nebulae were calculated using these solutions. For the planetaries contained in fields 1–10, the astrometric accuracy is limited to $\sim 1''$ by uncertainties in the Ford and Jacoby (1987b) and Ciardullo *et al.* (1987) secondary standards. Because of the lack of astrometric standards in the northeastern fields 11–13, the positions of planetaries in these fields may be somewhat more uncertain.

III. DEFINING THE STATISTICAL SAMPLE

Table 2 contains all 429 planetaries discovered on our images. This collection, however, is not a homogeneous

sample. In M31's inner regions, faint planetaries are lost in the bright background of the galaxy; thus the limiting magnitude of the survey is a function of position in the galaxy. Furthermore, for faint objects, photon noise affects whether or not an object is detected, again causing incompleteness. Hence, before any analysis could be attempted, a set of criteria had to be adopted to define a statistically complete and homogeneous sample.

One way of estimating the variation of incompleteness with galaxy surface brightness is through the calculation of the expected signal-to-noise ratio of an observation. By adding artificial stars onto an H α frame of M31's bulge, Ciardullo *et al.* (1987) found a linear relationship between the theoretical signal-to-noise of a detection and completeness: when a signal-to-noise of 9 was achieved, virtually all the objects were detected, but when the signal-to-noise dropped to 4, the frac-

TABLE 2—Continued

ID	$\alpha(1975)$	$\delta(1975)$	N	m_{5007}	s.e.(m)	Sample	ID	$\alpha(1975)$	$\delta(1975)$	N	m_{5007}	s.e.(m)	Sample
240	0 41 48.47	41 17 28.2	1	20.93	...		385	0 40 54.35	41 02 54.5	2	22.44	0.01	A
241	0 41 44.71	41 16 43.9	1	22.50	...		386	0 40 54.53	41 03 30.4	1	23.24	...	
242	0 41 52.03	41 13 47.8	2	22.29	0.05		387	0 40 56.43	41 06 44.2	1	20.77	...	
243	0 41 54.37	41 14 14.1	1	22.95	...		388	0 40 57.05	41 01 54.1	2	22.75	0.04	
244	0 42 01.06	41 15 39.3	2	22.29	0.03		389	0 40 57.88	41 07 21.8	1	22.51	...	
245	0 42 02.20	41 15 32.1	2	22.33	0.01		390	0 40 58.19	40 59 45.8	1	20.61	...	
246	0 42 01.94	41 15 04.0	2	22.61	0.06		391	0 40 58.22	41 04 28.9	2	22.59	0.01	A
249	0 42 05.14	41 16 36.9	1	23.41	...		392	0 40 58.71	41 03 15.5	2	23.41	0.11	
250	0 42 02.41	41 16 36.5	2	24.12	0.16		393	0 40 58.96	41 01 30.2	2	22.11	0.05	A
251	0 42 01.94	41 16 25.4	2	22.21	0.01		394	0 40 59.26	41 05 15.2	1	23.41	...	
252	0 41 54.35	41 18 15.5	1	21.75	...		395	0 40 59.49	41 01 42.0	1	21.59	...	AB
253	0 41 53.86	41 18 52.4	1	21.35	...		396	0 40 59.87	41 03 13.4	2	21.39	0.03	AB
254	0 41 47.43	41 18 39.8	1	22.36	...		397	0 40 59.98	41 04 49.7	1	22.81	...	
270	0 42 10.97	41 19 38.0	1	22.25	...		398	0 41 00.37	41 00 19.5	2	22.60	...	A
274	0 42 19.32	41 19 50.8	1	22.17	...		399	0 41 00.71	41 01 42.3	1	24.41	...	
275	0 42 15.49	41 19 27.0	1	22.90	...		400	0 41 00.97	41 05 24.9	1	21.99	...	AB
276	0 42 16.93	41 18 41.5	1	20.48	...		401	0 41 01.46	41 01 10.7	1	22.61	...	A
278	0 42 16.85	41 18 17.9	1	22.16	...		402	0 41 01.64	41 00 17.3	1	21.89	...	AB
279	0 42 10.27	41 18 04.8	2	23.11	0.01		403	0 41 01.77	41 02 57.8	2	23.45	0.03	
280	0 42 10.76	41 17 16.7	1	23.38	...		404	0 41 02.44	41 02 36.0	2	22.95	0.09	
281	0 42 15.63	41 16 21.8	2	21.52	0.01		405	0 41 02.49	41 08 33.3	1	23.78	...	
282	0 42 15.87	41 15 53.5	2	22.36	0.00		406	0 41 02.94	41 03 49.7	1	22.71	...	
283	0 42 18.21	41 15 18.2	1	22.12	...		407	0 41 03.24	41 03 48.0	1	22.90	...	
284	0 42 22.57	41 19 02.6	1	23.41	...		408	0 41 03.68	41 07 48.2	1	23.28	...	
285	0 42 20.97	41 19 19.1	1	22.86	...		409	0 41 03.70	41 02 53.4	2	22.83	0.03	
286	0 42 27.28	41 19 46.5	1	22.21	...		410	0 41 04.79	41 01 31.9	2	21.14	0.01	
287	0 42 30.74	41 19 46.0	2	22.65	0.04		411	0 41 05.38	41 06 49.1	1	23.67	...	
288	0 42 32.61	41 17 53.0	1	21.82	...		412	0 41 05.99	41 09 23.3	2	23.59	0.12	
291	0 40 56.44	41 07 48.4	1	22.66	...		413	0 41 06.10	41 01 43.5	2	21.21	0.01	
292	0 40 52.85	41 07 44.8	1	22.04	...		414	0 41 06.25	41 01 21.8	2	21.42	0.03	
293	0 40 53.72	41 08 04.8	1	22.52	...		415	0 41 06.42	41 07 01.2	2	23.21	0.02	
295	0 40 49.35	41 07 59.0	1	21.74	...		416	0 41 06.56	41 00 37.1	2	23.40	0.03	
296	0 40 48.29	41 07 53.0	1	23.05	...		417	0 41 06.58	41 07 22.1	2	23.04	0.08	
316	0 41 21.96	41 07 50.8	2	23.31	0.09		418	0 41 06.64	41 01 44.6	2	23.19	0.05	
323	0 41 22.96	41 07 16.8	1	22.17	...		419	0 41 06.74	41 03 24.6	2	22.36	0.02	
328	0 41 27.09	41 07 59.6	3	22.49	0.07		420	0 41 08.05	41 05 55.2	1	23.36	...	
330	0 41 27.30	41 08 37.6	3	22.13	0.01		421	0 41 08.49	41 09 40.5	1	23.48	...	
372	0 40 46.11	41 01 54.7	1	23.44	...		422	0 41 09.10	41 02 16.6	2	22.68	0.04	
373	0 40 47.58	41 03 42.3	1	22.29	...	A	423	0 41 09.10	41 06 12.7	1	23.03	...	
374	0 40 48.11	41 00 38.5	2	22.83	0.05		424	0 41 09.74	41 09 19.5	2	23.18	...	
375	0 40 48.09	41 04 25.5	1	20.58	...	AB	425	0 41 10.15	41 10 15.5	1	23.71	...	
376	0 40 48.55	41 02 27.7	2	23.01	0.03		426	0 41 11.69	41 01 55.9	2	23.01	0.01	
377	0 40 48.88	40 59 51.8	1	23.18	...		427	0 41 11.90	41 08 35.7	2	22.98	0.11	
378	0 40 50.38	41 05 13.1	1	21.65	...	AB	428	0 41 11.87	41 08 18.4	1	22.59	...	
379	0 40 50.97	41 01 41.7	2	23.66	0.12		429	0 41 12.27	41 01 02.4	2	22.75	0.03	
380	0 40 51.66	41 05 24.2	1	20.28	...	AB	430	0 41 12.74	41 00 03.0	1	22.92	...	
381	0 40 51.68	41 00 45.3	1	23.47	...		431	0 41 12.95	41 09 15.1	2	23.05	0.04	
382	0 40 53.53	41 04 30.9	1	22.90	...		432	0 41 13.48	41 10 10.6	1	23.64	...	
383	0 40 53.69	41 01 17.5	2	23.57	0.08		433	0 41 13.54	41 05 37.4	2	22.53	0.04	A
384	0 40 54.30	41 02 31.6	1	24.15	...		434	0 41 14.80	41 10 09.9	1	24.05	...	

tion of objects found approached zero. This same rule can be applied to the $\lambda 5007$ observations. By using M31's observed luminosity profile (Kent 1987), and scaling Ciardullo *et al.*'s (1987) net system throughput to that expected for the CCD and $\lambda 5007$ filter, the completeness at any isophote can be computed (cf. eq. [5] of Ciardullo *et al.* 1987). From this analysis, the sample of PNs should be complete to ~ 22.8 mag for isophotal distances greater than $90''$ from M31's nucleus; if objects as close as $15''$ from the nucleus are included, the completeness limit should only be ~ 22.1 . Therefore, to remove the effects of incompleteness, two samples were defined: for the analyses of the entire PNLf, all objects closer than $90''$ from the nucleus were excluded and $m_{5007} = 22.7$ was adopted as the magnitude completeness limit; for work concentrating on the bright end of the planetary nebula luminosity function, however, objects with isophotal distances as close as $15''$ from

M31's nucleus were included, but the magnitude limit of the sample was set at $m_{5007} = 22.0$. As can be seen in Figure 2, these are conservative limits; the observed luminosity function formed from all the data does not turn over until $m_{5007} > 23$. Still, by staying comfortably above these thresholds, we ensure that none of our conclusions are biased by sampling errors.

A second source of uncertainty in the PNLf is caused by extinction. This comes from two sources. Because M31 has such a large angular size on the sky, the extinction due to dust in our own Galaxy changes significantly with position in M31. Fortunately, this is not a problem in our sample, since our survey region extends only $\sim 40'$ in length. The more serious contamination comes from the dust internal to M31. Because our survey was aimed primarily at M31's bulge, the areas of M31 which have the heaviest obscuration, the spiral arms and the disk, have in large been avoided. However, small patches of

TABLE 2—Continued

ID	$\alpha(1975)$	$\delta(1975)$	N	m_{5007}	s.e.(m)	Sample	ID	$\alpha(1975)$	$\delta(1975)$	N	m_{5007}	s.e.(m)	Sample
435	0 41 15.19	41 00 56.6	2	23.66	0.09		485	0 41 37.88	41 13 21.8	1	23.23	...	
436	0 41 15.28	41 05 25.7	1	22.97	...		486	0 41 38.01	41 08 40.9	1	23.44	...	
437	0 41 15.90	41 01 42.7	1	22.54	...	A	487	0 41 38.98	41 18 07.9	1	23.70	...	
438	0 41 16.11	41 01 46.1	2	22.31	0.03	A	488	0 41 39.34	41 10 21.3	1	23.54	...	
439	0 41 16.30	41 03 05.2	2	22.78	0.06		489	0 41 40.26	41 08 47.7	3	22.83	0.08	
440	0 41 16.43	41 05 57.1	1	22.68	...	A	490	0 41 40.30	41 16 02.3	1	23.48	...	
441	0 41 16.75	41 05 46.7	1	23.07	...		491	0 41 40.67	41 17 58.6	1	22.79	...	
442	0 41 17.30	41 08 07.3	2	21.54	0.05	B	492	0 41 41.56	41 13 12.2	1	22.99	...	
443	0 41 17.76	41 07 39.1	1	22.33	...		493	0 41 42.26	41 06 30.9	1	22.85	...	
444	0 41 18.15	41 03 20.9	2	22.69	0.02		494	0 41 44.05	41 11 01.5	1	23.80	...	
445	0 41 18.35	41 09 11.9	1	22.70	...		495	0 41 44.09	41 09 38.3	1	23.34	...	
446	0 41 18.47	41 04 14.4	1	23.63	...		496	0 41 45.62	41 07 18.0	1	23.73	...	
447	0 41 19.05	41 10 08.2	2	22.87	0.36		497	0 41 45.58	41 07 35.0	1	23.30	...	
448	0 41 19.18	41 09 59.5	1	22.57	...	A	498	0 41 45.63	41 07 25.4	1	22.89	...	
449	0 41 19.25	41 06 49.0	2	22.80	0.12		499	0 41 45.83	41 09 29.9	1	23.41	...	
450	0 41 20.59	41 01 34.2	2	22.10	0.04		500	0 41 47.13	41 13 42.1	1	24.42	...	
451	0 41 21.64	41 00 47.6	2	22.53	0.01		501	0 41 50.08	41 15 34.6	1	23.90	...	
452	0 41 21.73	41 05 16.4	1	23.17	...		502	0 41 50.57	41 08 31.3	1	22.37	...	A
453	0 41 22.23	41 10 00.8	1	23.50	...		503	0 41 52.78	41 13 28.4	2	25.87	0.37	
454	0 41 23.52	41 07 48.2	2	22.14	0.04		504	0 41 52.99	41 10 15.8	1	23.18	...	
455	0 41 23.74	41 10 12.5	1	23.09	...		505	0 41 56.35	41 07 27.4	1	22.79	...	
456	0 41 24.96	41 03 20.2	1	23.05	...		506	0 41 57.17	41 11 03.7	1	23.34	...	
457	0 41 25.04	41 03 27.2	1	23.22	...		507	0 41 57.26	41 10 54.6	1	22.22	...	A
458	0 41 25.32	41 03 14.8	1	23.20	...		508	0 41 59.01	41 15 07.5	1	25.28	...	
459	0 41 25.34	41 12 48.8	1	22.74	...		509	0 41 59.17	41 11 35.2	1	23.32	...	
460	0 41 25.95	41 09 21.6	4	22.73	0.10		510	0 42 01.17	41 15 35.0	1	26.79	...	
461	0 41 26.04	41 07 41.7	1	22.93	...		511	0 42 02.33	41 12 12.4	2	22.82	0.06	
462	0 41 28.22	41 07 43.6	3	21.79	0.03		512	0 42 03.45	41 14 28.7	1	22.96	...	
463	0 41 28.23	41 07 22.0	3	22.95	0.09		513	0 42 05.72	41 14 48.6	1	24.50	...	
464	0 41 28.28	41 10 22.8	1	23.32	...		514	0 42 08.09	41 16 55.0	1	23.78	...	
465	0 41 28.49	41 09 23.7	4	22.00	0.05		515	0 42 08.84	41 19 17.5	1	24.03	...	
466	0 41 29.40	41 07 51.2	1	23.27	...		516	0 42 11.30	41 13 52.8	1	24.22	...	
467	0 41 29.73	41 08 53.0	1	23.11	...		517	0 42 12.32	41 14 44.7	1	26.05	...	
468	0 41 29.92	41 07 40.7	1	22.99	...		518	0 42 13.02	41 14 18.0	1	21.63	...	
469	0 41 30.30	41 09 01.0	1	22.71	...		519	0 42 14.60	41 15 24.0	1	23.29	...	
470	0 41 30.55	41 08 34.5	3	23.16	0.09		520	0 42 14.88	41 14 26.0	1	22.04	...	
471	0 41 30.53	41 09 03.2	1	24.08	...		521	0 42 15.01	41 15 42.4	2	23.37	0.05	
472	0 41 31.42	41 05 47.5	1	23.26	...		522	0 42 17.00	41 14 45.7	1	21.86	...	
473	0 41 31.62	41 08 49.5	3	23.08	0.05		523	0 42 20.06	41 14 35.2	1	23.61	...	
474	0 41 31.79	41 06 52.0	2	22.94	0.05		525	0 42 22.82	41 15 43.4	2	24.12	0.04	
475	0 41 31.90	41 05 24.5	1	23.40	...		526	0 42 32.68	41 17 57.6	1	24.03	...	
476	0 41 31.94	41 06 04.8	2	23.20	0.09		527	0 42 34.83	41 19 05.9	2	22.93	0.13	
477	0 41 32.79	41 08 49.6	2	23.03	0.02		528	0 42 35.81	41 16 18.1	1	23.10	...	
478	0 41 32.98	41 08 59.7	2	22.68	0.11	A	529	0 42 35.99	41 22 34.7	1	23.53	...	
479	0 41 33.37	41 17 36.9	1	23.02	...		530	0 42 36.42	41 19 08.3	2	22.19	0.03	
480	0 41 34.08	41 10 41.4	1	23.50	...		531	0 42 37.26	41 18 04.8	1	23.38	...	
481	0 41 34.63	41 06 18.3	1	23.97	...		532	0 42 40.26	41 19 52.9	2	21.63	0.02	
482	0 41 34.80	41 07 22.9	1	23.25	...		533	0 42 40.63	41 23 06.6	1	24.19	...	
483	0 41 36.16	41 06 53.8	2	23.59	0.03		534	0 42 42.04	41 23 08.3	1	24.23	...	
484	0 41 37.27	41 11 50.8	1	23.71	...		535	0 42 43.72	41 17 49.2	1	23.26	...	

dust do exist in the region, and have been identified both by unsharp masking techniques (Johnson and Hanna 1972 and Hodge 1980; Gallagher and Hunter 1981; McElroy 1983) and by color (Kent 1983; Ciardullo *et al.* 1988). While it is impossible to correct completely for this internal extinction without a detailed spectroscopic study of each object, subsamples of the planetaries lying in relatively unobscured regions of the galaxy can be defined. In order to do this, the positions of the planetary nebulae were superposed upon an extremely high contrast display of the $B - \lambda 6200$ color map of Ciardullo *et al.* (1988). Those objects which were projected onto areas 0.025 mag redder than the apparent color of the bulge, or which fell outside the region included in the color map, were excluded from the samples.

Unfortunately, color maps are not always the optimal way

of discovering dust. When dust is embedded in a galaxy, starlight emitted foreground to the obscuration will dilute any reddening which may occur. For example, a dust patch with an intrinsic differential extinction of $E(B - V) = 0.39$, if located in the center of a galaxy, will cause an observer to measure a $B - V$ color which is 0.08 mag redder than the surroundings. Any additional dust in the cloud only makes the area appear bluer, since the additional extinction reduces the relative contribution of the reddened light and allows the color of the foreground stars to dominate. Therefore, in order to avoid the effects of dust clouds embedded deep in M31's bulge, a technique is needed which is sensitive to total rather than differential obscuration. Such a technique is the method of enhancing faint structures with unsharp masking.

Unsharp pictures of M31's bulge have existed for some time

TABLE 2—Continued

ID	$\alpha(1975)$	$\delta(1975)$	N	m_{5007}	s.e.(m)	Sample	ID	$\alpha(1975)$	$\delta(1975)$	N	m_{5007}	s.e.(m)	Sample
536	0 42 44.47	41 19 55.2	2	22.65	0.04		554	0 42 57.39	41 22 10.7	1	23.69	...	
537	0 42 44.96	41 17 21.2	1	21.20	...		555	0 43 02.14	41 21 36.4	1	20.64	...	
538	0 42 45.44	41 22 30.2	1	24.19	...		556	0 43 02.25	41 22 16.6	2	23.78	0.03	
539	0 42 45.89	41 23 08.6	1	22.59	...		557	0 43 02.68	41 23 35.7	1	21.27	...	
540	0 42 46.01	41 18 57.8	2	23.88	0.05		558	0 43 03.15	41 21 42.9	1	22.20	...	
541	0 42 47.29	41 19 01.5	2	21.44	0.02		559	0 43 04.04	41 25 05.0	1	20.48	...	
542	0 42 48.76	41 23 18.1	1	24.03	...		560	0 43 07.53	41 24 35.2	1	21.57	...	
544	0 42 50.09	41 23 04.0	1	24.53	...		561	0 43 07.89	41 24 25.8	1	23.83	...	
545	0 42 50.90	41 21 59.4	1	21.80	...		562	0 43 08.67	41 25 31.8	1	23.92	...	
546	0 42 52.30	41 19 53.8	1	23.69	...		563	0 43 12.26	41 25 19.5	1	20.89	...	
547	0 42 52.79	41 20 56.1	1	23.86	...		564	0 43 16.51	41 23 21.4	1	22.56	...	
548	0 42 53.22	41 19 05.0	1	21.90	...		565	0 43 17.25	41 24 59.8	1	23.49	...	
549	0 42 53.91	41 23 08.3	2	23.60	0.09		566	0 43 19.39	41 23 54.2	1	22.03	...	
550	0 42 54.78	41 21 38.1	1	22.60	...		567	0 43 22.92	41 23 39.8	1	21.95	...	
551	0 42 55.41	41 25 32.5	1	21.76	...		568	0 43 27.80	41 22 58.1	1	20.62	...	
552	0 42 55.58	41 22 01.6	1	23.55	...		569	0 43 27.99	41 23 41.1	1	21.69	...	
553	0 42 56.80	41 18 56.6	1	24.01	...								

(Johnson and Hanna 1972; McElroy 1983). However, because of the difficulty involved in comparing these pictures accurately with the positions of our several hundred planetaries, these reproductions were not used. Instead, we created our own digital unsharp mask by applying an 8"1 FWHM Gaussian filter to Ciardullo *et al.*'s (1988) *B* image of M31's central region. This mask was then divided into the original, enabling a comparison of the locations of the dust features with the planetary nebula positions. As a result of this comparison, seven additional PNs were excluded from our samples.

After correcting for incompleteness and possible dust obscuration, 104 PNs brighter than $m_{5007} = 22.7$ remained in our complete sample. These are marked in Table 2 with the letter A. The 76 planetaries marked in Table 2 with the letter B comprise the complete set of bright planetaries, with $m_{5007} < 22.0$.

IV. THE SHAPE OF THE PLANETARY NEBULA LUMINOSITY FUNCTION

Figure 3 displays the observed PNLf derived from the sample of bright planetaries (sample B described above). Immediately obvious from the figure is that, for the brightest

planetaries, the luminosity function is not a power law—there is a rapid falloff which is potentially an excellent standard candle. In fact, as Figure 2 suggests, $N(m)$ for the top 0.5 mag is very nearly a line, with an intercept at $m_{5007} \approx 20.2$. At apparent magnitudes fainter than $m_{5007} = 20.8$, however, the curve flattens, and is more like the luminosity function found by Jacoby (1980) for planetaries in the Magellanic Clouds.

The solid line in Figure 3 shows Paper I's theoretical luminosity function derived from an ensemble of helium-burning central stars with a mean mass of $0.61 M_{\odot}$ and a Gaussian dispersion of $0.02 M_{\odot}$. In order to compare the model's absolute fluxes to the apparent magnitudes of M31's planetaries, both a distance and an estimate for the total λ_{5007} extinction toward M31 were needed. For the distance to M31, we adopted Welch *et al.*'s (1986) value of 710 kpc, which is based on the infrared photometry of Cepheids. This value is in good agreement with the RR Lyrae-based distance determination of 740 kpc (Pritchett and van den Bergh 1987), and the halo giant distance estimate of 760 kpc (Mould and Kristian 1986). To correct for extinction, we combined Seaton's (1979) Galactic extinction law with McClure and Racine's (1969) estimate of $E(B - V) = 0.11$ for the differential extinction in the direction of M31's bulge. The resulting apparent distance modulus of $(m - M) = 24.65$ was then used to shift the theoretical curve onto Figure 3. Despite the limitations in the models, at the bright end of the luminosity function the predicted falloff is in good agreement with the observations. The PNLf of M31 clearly supports the idea of a firm upper limit on the [O III] luminosity of planetary nebulae. This behavior can be most easily explained as arising from a sharp cutoff in the upper mass limit of planetary nebula central stars in combination with extremely rapid evolutionary time scales for more massive candidate progenitors (Paper I).

Although the completeness limit of the observations extends only ~ 2.5 mag, it is possible to estimate the shape of the entire PNLf by combining these results with those found by Jacoby (1980) for the Magellanic Clouds. According to Jacoby, the faint end of the PNLf agrees with the theoretical luminosity function of Henize and Westerlund (1963) in which a planetary nebula is idealized as a uniformly expanding homogeneous gas sphere ionized by a nonevolving central star. The data from M31 suggest, however, that at the bright end of the luminosity function, the evolution of the central star is important, as is the

TABLE 3
UNCONFIRMED PLANETARY NEBULAE FROM
FORD AND JACOBY 1978

Identification	This Survey
4	Not seen
11	Not seen
19	Not seen
22	Not seen
73	Not seen
88	Seen in continuum
96	Seen in continuum
108	Not seen
146	Not seen
158	Not seen
185	Not seen
187	Not seen
190	Seen in continuum
191	Seen in continuum
193	Not seen
194	Not seen
294	Not seen

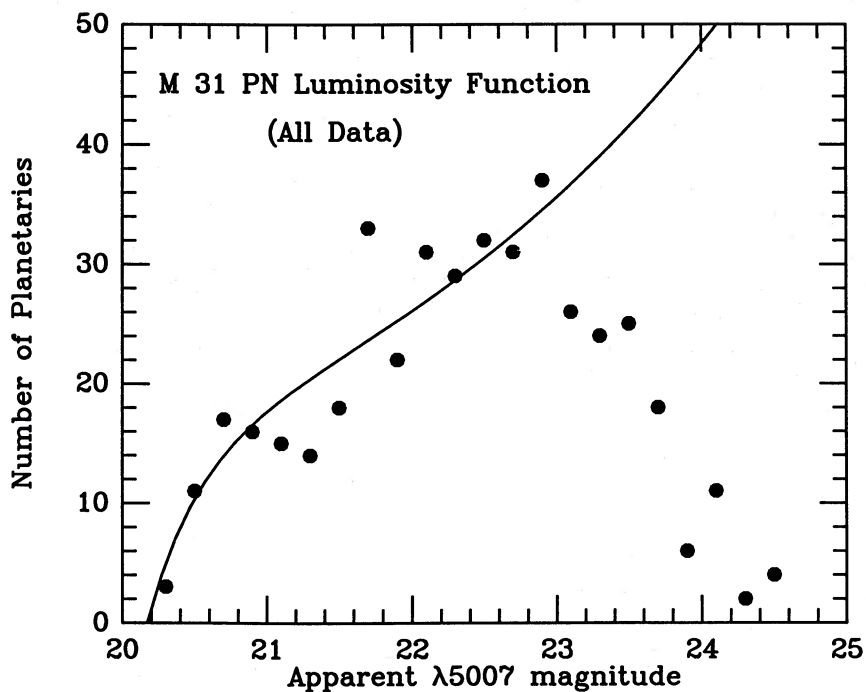


FIG. 2.—M31's PNLF derived using all the data, regardless of position in the galaxy or internal reddening. The data have been binned into 0.2 mag intervals. The solid line is a modified Henize and Westerlund (1963) model luminosity function, with a magnitude cutoff at $m^* = 20.17$. The falloff at magnitudes $m_{5007} > 23$ is due to incompleteness.

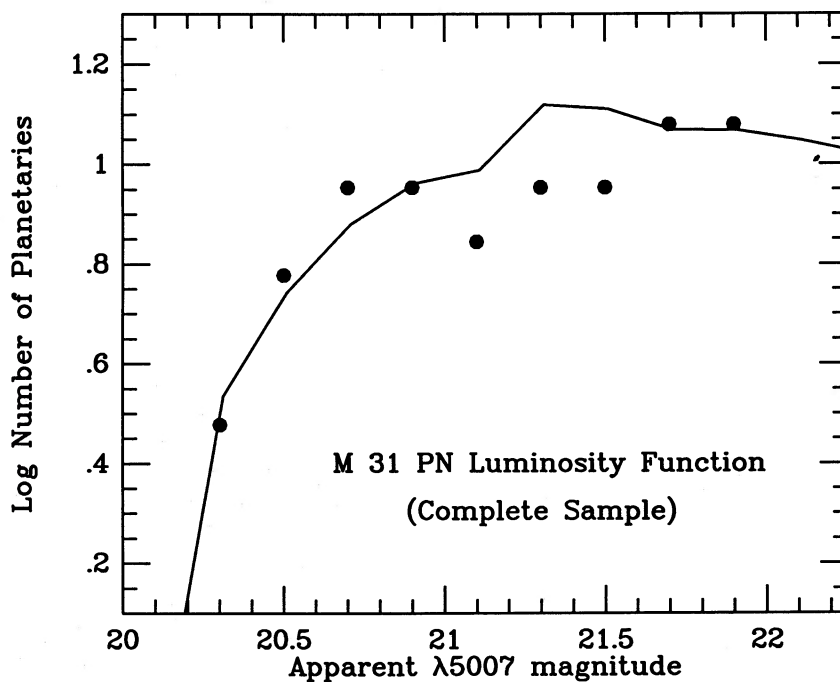


FIG. 3.—M31's PNLF derived from a homogeneous sample of PNs with $m_{5007} < 22.0$ located in relatively dust-free regions of the bulge. The data have been binned into 0.2 mag intervals and plotted in log space. The solid line is the theoretical curve of Jacoby (1989) created from a set of PN central star evolutionary models with a mean mass of $M = 0.61 M_{\odot}$ and a variance of $\sigma(M) = 0.02 M_{\odot}$. For the brightest PNs the luminosity function is clearly not a power law, supporting the use of planetaries as standard candles.

distribution of central star masses. Consequently an accurate representation of the true PNLF requires two components: one which models the envelope expansion and slow PN fade rate, and another which reproduces the high mass cutoff. A formulation which combines the simple Henize and Westerlund (1963) model with a sharp exponential truncation is given below:

$$N(M) \propto e^{0.307M}(1 - e^{3(M^* - M)}). \quad (2)$$

Figure 4 combines the two samples of M31 planetaries and compares the observed luminosity function with a fit to equation (2). This empirical PNLF is also plotted in Figure 2.

Paper I has shown that the [O III] $\lambda 5007$ luminosity expected from a planetary nebula is rather insensitive to metallicity, since the emitted flux goes only as the square root of the oxygen abundance. A subsequent paper on the NGC 3379 group (Ciardullo, Jacoby, and Ford 1989) will show that the rapid decline at the bright end of the PNLF appears to be the same in all early-type galaxies. This being the case, the value M^* , as defined, represents the absolute $\lambda 5007$ magnitude of the brightest planetary nebula which can exist in any galaxy. It is thus, a standard candle. From Figure 4, the apparent magnitude of m^* in M31 is $m_{5007} = 20.17$. Applying the foreground extinction described above, and adopting 710 kpc as the distance to M31, this limit is equivalent to an absolute $M^* = -4.48$.

V. THE SPECIFIC PLANETARY NEBULA DENSITY

From stellar evolution theory, it is expected that the luminosity-specific stellar death rate of a galaxy should be invariant to the precise state of the underlying stellar population. Renzini and Buzzoni (1986) have shown that this quantity is remarkably independent of both age and initial mass

function: for populations older than $\sim 10^9$ yr, this number varies by less than a factor of ~ 1.6 , and under no circumstances does it change by more than a factor of 5. Since a large majority of the stars in any old or intermediate-age stellar population become planetary nebulae, this constancy in the stellar death rate should be equivalent to an invariance in the rate of planetary nebula production. If this is the case, the number density of planetaries per unit bolometric luminosity should be approximately the same in every galaxy.

There is some evidence that this is indeed the case. From the number of planetaries detected in their image-tube fields, Ford and Jacoby (1978a) concluded that the ratio of PNs per unit B light in M31's bulge and inner disk must not change much with radius. Ford *et al.* (1988) demonstrated a similar invariance in NGC 5128, where over 200 PNs have been detected at radial distances between 5 and 20 kpc. In a comparison of planetary nebula densities in different galaxies, Jacoby (1980) estimated that the number of PNs per unit V luminosity in Local Group galaxies is constant to within a factor of 3. Although our present planetary nebula survey was directed primarily at M31's bulge, the outermost fields sample enough of the disk so that it is possible to test for any large discrepancy in the luminosity-specific number density of planetaries.

In order to estimate the PN radial distribution, the Gunn r -band surface photometry of Kent (1987) was used to model M31 as a series of concentric elliptical isophotes with varying axial ratios and position angles. The isophotal radial distance of each planetary was calculated by finding the semimajor axis of the isophote upon which it was superposed. The distribution of these distances was then compared with the luminosity along M31's major axis corrected for the fraction of light covered in our survey.

Figure 5 compares the differential radial distribution of

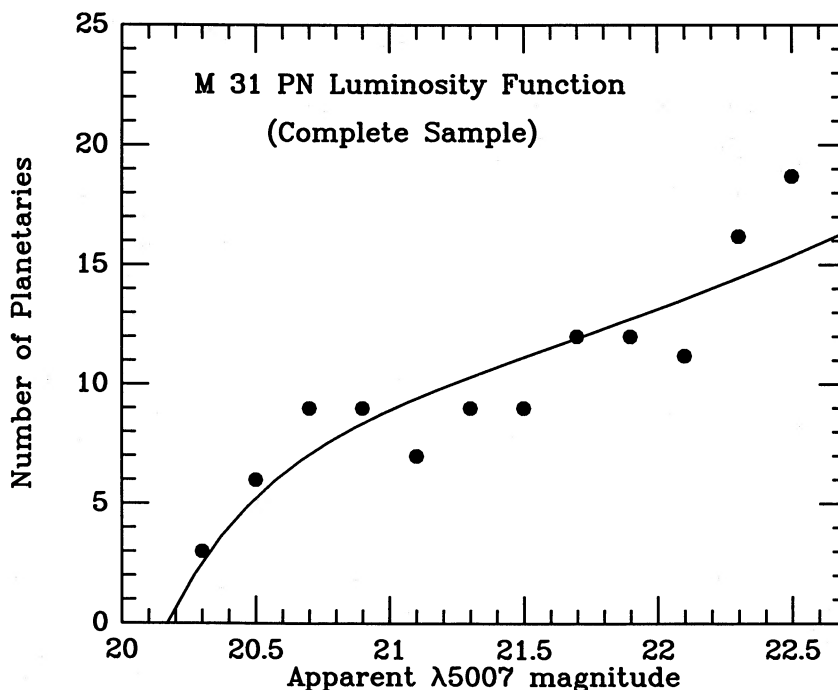


FIG. 4.—M31's PNLF derived from a homogeneous sample of planetaries plotted against a modified Henize and Westerlund (1963) model. The data have been binned into 0.2 mag intervals. The apparent PN magnitude cutoff is $m^* = 20.17$, which translates into $M^* = -4.48$. A comparison with Fig. 2 shows that the presence of a small amount of dust does not severely disturb the shape or magnitude cutoff of the observed PNLF.

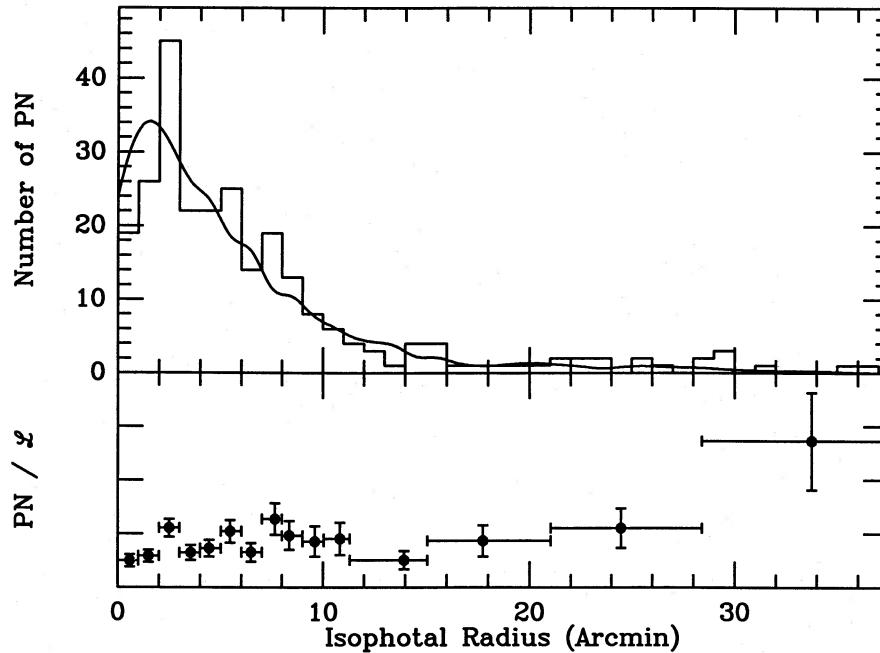


FIG. 5.—Distribution of the isophotal radii of M31 planetaries. In the top panel the solid line displays the amount of light contained in the survey region vs. isophotal radius. The bottom panel gives the variation of the luminosity-specific PN number density. There is no significant difference in this PN density between M31's bulge and inner disk.

planetaries to that portion of M31's light sampled in our 13 survey fields. In order to sample as much of the disk as possible, as well as test the assumptions about incompleteness detailed in § III, all planetaries brighter than $m_{5007} = 22.7$ have been included in the histogram. Two properties are immediately obvious from the figure. First, as expected, incompleteness is important in the central regions, as evidenced by a decrease in the luminosity-specific number density of planetaries within the central arcminute. Second, although the amount of luminosity sampled at large radii is small, there is no evidence for a difference in the specific number density of planetary nebulae between M31's bulge and disk. When normalized to the background luminosity, the rate of planetary nebular production and hence the stellar death rate appear to be the same in both M31's bulge and its inner disk populations.

If indeed, the luminosity-specific stellar death rate is invariant, then the number of planetaries per unit luminosity is an important quantity, both as a distance indicator (Jacoby and Lesser 1981) and as a check on stellar evolution theory. Unfortunately, M31 is not the ideal place to perform this measurement, since its irregular internal extinction can alter the PNLF and decrease the number of bright planetaries detected. Nevertheless, by confining the calculation to a region of M31's bulge

which is relatively dust-free, an estimate for a lower limit on the luminosity-specific planetary nebula number density can be made.

Although a few small dust patches can be seen in M31's bulge, an examination of the Ciardullo *et al.* (1988) color map shows that the worst areas of extinction originate in M31's inner spiral arm, which projects a few arcminutes northwest and southeast of the nucleus. Hence, for the calculation of PN densities, these regions and fields further into M31's disk were excluded. When combined with the necessity of excluding the area immediately surrounding M31's nucleus, this left two regions of interest. For determining the density of planetaries 0.5, 1, and 1.5 mag down M31's PNLF, only the annulus between $15'' < r_{\text{iso}} < 285''$ from M31's nucleus was included in the calculation. When counting planetaries to fainter levels, the region of interest was further constrained to isophotal distances between $90'' < r_{\text{iso}} < 285''$.

Table 4 gives the number density of bright planetaries found in M31 per unit B , V , R , and bolometric light. The absolute bolometric magnitudes quoted in the table were computed in the following manner. After calculating the integrated apparent V -magnitudes of the survey annuli using the photometry and transformations of Kent (1987), corresponding absolute

TABLE 4
M31 LUMINOSITY-SPECIFIC PLANETARY NEBULA DENSITIES

$(M^* - M)$	Number of PNs	m_V	M_{bol}	$\text{PN}/(L_B)_\odot$ ($\times 10^{-9}$)	$\text{PN}/(L_V)_\odot$ ($\times 10^{-9}$)	$\text{PN}/(L_R)_\odot$ ($\times 10^{-9}$)	$\text{PN}/(L_{\text{bol}})_\odot$ ($\times 10^{-9}$)
0.5.....	10	5.31	-20.09	2.9	2.2	1.9	1.2
1.0.....	33	5.31	-20.09	9.4	7.4	6.3	3.9
1.5.....	58	5.31	-20.09	16.6	13.0	11.1	6.9
2.0.....	68	5.72	-19.68	28.4	22.3	19.0	11.8
2.5.....	94	5.72	-19.68	39.3	30.8	26.3	16.3

magnitudes were found by correcting for M31's $E(B-V) = 0.11$ extinction and assuming a distance of 710 kpc (cf. § IV). The spectral energy distribution of M31's bulge was then estimated by combining the UV and optical energy distribution of Coleman, Wu, and Weedman (1980) with the infrared photometric magnitudes of Sandage, Becklin, and Neugebauer (1969). Similarly, a set of stellar energy distributions was created by merging optical spectra (Jacoby, Hunter, and Christian 1984) with ultraviolet spectra (Wu *et al.* 1983) and infrared magnitudes (Johnson 1966) for late-type stars with equivalent spectral types. A bolometric correction applicable to M31's bulge was then calculated by comparing M31's V bandpass flux with its total emitted flux, and normalizing this number to the corresponding values obtained for the stars. The resulting bolometric correction, -0.80 mag (similar to that of a late K star), was then added to the absolute V -magnitudes to yield the bolometric magnitudes of the survey regions.

The luminosity-specific PN number density listed in Table 4 for B light is in very good agreement with that found by Nolthenius and Ford (1987) in M31's outer disk and halo. For PNs within 2.36 mag of M^* , our data imply a $\text{PN}/(L_B)_\odot$ value of 3.6×10^{-8} . This compares well with the value of $\sim 3.8 \times 10^{-8}$ derived from Nolthenius and Ford's data for PNs with projected distances between 15 and 20 kpc. This agreement is added support for the constancy of the luminosity-specific PN density.

It should be emphasized here that the numbers tabulated in Table 4 are lower limits, since, as detailed above, some dust does exist in M31's bulge. A total of 49 bright planetaries ($m_{5007} < 22.0$) project onto the southwest (near side) of M31's bulge, while only 31 are located on the far side. For the fainter sample of planetaries, the discrepancy is found in the same direction, although the amplitude is much less: 53 PNs are found on the near side, compared with 45 on the far side. This asymmetry can most easily be explained by assuming that dust, located in or near the plane of M31, is affecting the observed magnitudes of background PNs. Although small amounts of dust may not affect the shape of the PNLF dramatically (compare the luminosity functions of Figs. 2 and 4), it will cause the total PN population to be underestimated.

The data in Table 4 were also extrapolated to place a lower limit on the specific stellar death rate. First, the 98 planetaries between $90'' < r_{\text{iso}} < 285''$ which have magnitudes brighter than the completeness limit of $m_{5007} = 22.7$ were used to define the constant of proportionality of equation (2). This equation was then integrated down 8 mag from M^* , thereby accounting for the faintest known Galactic planetary, and yielding ~ 970 for the total number of planetaries in that portion of M31's bulge. Dividing this number by a mean PN lifetime of 25,000 yr (Pottasch 1984) and normalizing to the bolometric luminosity sampled then results in a luminosity-specific stellar death rate of $\sim 5.7 \times 10^{-12}$ stars $\text{yr}^{-1} L_\odot^{-1}$. This is roughly a factor of 3 less than the theoretical death rate derived by Renzini and Buzzoni (1986). Considering that (1) the PN densities in Table 4 represent lower limits, (2) a 5 mag (factor of ~ 10) extrapolation was performed, and (3) some stars never enter the PN phase (Schönberner 1983; Kudritzki, Mendez, and Simon 1983; Heber *et al.* 1983; Drilling and Schönberner 1983), our observed stellar death rate is in good agreement with the models. Note that this rate, when combined with a Galactic $M_V = -20.6$ (de Vaucouleurs and Pence 1978) implies a PN population in the Galaxy of ~ 4000 .

VI. THE PLANETARY NEBULA LUMINOSITY FUNCTION AS A STANDARD CANDLE

The most common method of comparing an observational luminosity function with a model is to bin the results, correct for observational uncertainty with the Eddington (1913) expansion, and fit the resulting histogram using the method of least squares. When the number of objects observed is large, there is no problem with this procedure. However, as the number of objects decreases, the effects of the finite bin size become more pronounced. One is faced with the problem of choosing bins large enough to overcome the errors of poor counting statistics, yet narrow enough to contain magnitude information. At Virgo Cluster distances, the number of detectable planetaries is small enough so that the process of binning reduces the accuracy of any distance determination.

An alternative and superior way of fitting an observational luminosity function is through the method of maximum likelihood (Hanes and Whittaker 1987). In this technique, the underlying universal luminosity function, $\phi(M)$, is treated as a probability distribution function; hence, if Poisson statistics hold, the probability of observing n planetaries in any magnitude interval is

$$p(n) = \frac{[\lambda(M)dM]^n e^{-\lambda(M)dM}}{n!}, \quad (3)$$

where $\lambda(M)$ is the number of planetaries expected from the true luminosity function. In the limit where the magnitude interval dM becomes infinitesimal, each bin contains either zero or one object, and the net probability of observing a given distribution $\phi(m)$ is

$$P = \exp \left[- \int_{-\infty}^{m_i - \mu} \alpha \times 10^{0.4(C + \mu - m_{\text{gal}})} \phi(m) dm \right] \times \prod_{i=1}^N \alpha \times 10^{0.4(C + \mu - m_{\text{gal}})} \phi(m_i - \mu) dm, \quad (4)$$

where α is the luminosity-specific number density of planetaries, m_{gal} is the integrated galaxy magnitude in the survey region, N is the number of PNs detected, m_i is the completeness limit of the sample, C is the constant defining the bolometric magnitude scale zero point, and μ is the apparent distance modulus ($m - M$). The condition of maximum likelihood dictates that the partial derivatives of $\ln P$ with respect to the independent variables α and μ be zero; therefore, by differentiating with respect to these variables and combining the results, the following "best-fit" condition for the distance μ can be derived:

$$\sum_{i=1}^N \frac{1}{\phi(m_i - \mu)} \frac{\partial}{\partial \mu} [\phi(m_i - \mu)] = N \frac{\partial}{\partial \mu} \left[\frac{\int_{-\infty}^{m_i - \mu} \phi(m) dm}{\int_{-\infty}^{m_i - \mu} \phi(m) dm} \right]. \quad (5)$$

Once μ is found, the distance to the galaxy follows directly after correcting for the interstellar extinction A_{5007} . This equation can be used for objects of any type as long as they are drawn from a known luminosity function.

If the number of planetaries per unit luminosity is truly invariant as suggested by theory, the maximum-likelihood condition is further constrained, since α is then a constant.

Under these circumstances, the distance modulus μ becomes the lone free parameter, and the best-fit condition becomes

$$\sum_{i=1}^N \frac{1}{\phi(m_i - \mu)} \frac{d}{d\mu} [\phi(m_i - \mu)] + 0.921N \\ = \alpha \times 10^{0.4(C + \mu - m_{\text{gal}})} \left[0.921 \int_{-\infty}^{m_i - \mu} \phi(m) dm \right. \\ \left. + \frac{d}{d\mu} \int_{-\infty}^{m_i - \mu} \phi(m) dm \right]. \quad (6)$$

Note that, from § V, it is the bolometric magnitude of the galaxy which is used by theorists in their models. Hence, to use equation (6) properly, m_{gal} must represent the apparent bolometric magnitude of the galaxy corrected for the effects of interstellar extinction.

Although the above formulations are useful, two additional complications must be considered. The first is that nowhere in the above analysis do the effects of observational error enter. In the conventional least-squares fit, the uncertainty in the value of each bin can either be included directly in the maximum-likelihood estimator or be used to perform a deconvolution in the count distribution (Eddington 1913). In the above analysis, however, since binning is not done, neither of these solutions is possible. Instead, the converse operation must be performed. Before comparing the observed luminosity function with that of a model, the model must be modified to predict what the measurement uncertainties will do to the observations. This requires a convolution of the measurement error profile (usually assumed to be Gaussian) with the underlying luminosity function. Because the error term changes with signal-to-noise (especially near the frame limit), the width of the convolution filter must also change with magnitude. In practice, this means that the shape of the theoretical probability distribution function, ϕ , is a function of the distance modulus, and therefore the function, its integral, and its derivative must be recalculated for every value of μ .

A second consideration is that the above equations require that the limiting magnitude be known. This is never the magnitude of the faintest planetary; far before this limit is encountered, incompleteness becomes important. In principle, the incompleteness as a function of signal-to-noise can be estimated from known quantities (cf. Ciardullo *et al.* 1987), and a correction factor can be applied to the theoretical probability distribution function. In reality, however, this is extremely dangerous, since a small error can lead to a very wrong result. Instead, an estimate of the true completeness limit should be made from an examination of the binned magnitude counts, and all planetaries fainter than this limit disregarded.

Equations (5) and (6) yield the most probable value of the distance, but they do not assign an error to that value or test how well the observed luminosity distribution agrees with the theoretical function. The former task, that of placing formal confidence limits on a given result, can most easily be performed through equation (4). In the case of a variable PN density, probability contours in (α, μ) -space can be calculated, enabling the variation of μ with α to be directly examined. If α is held constant, of course, these probability contours become one-dimensional curves and can be displayed with simple error bars.

The maximum-likelihood formulations described above do not address the question of whether the PNLf is universal or whether the observed PNLf of a galaxy agrees with a previously derived luminosity function. Fortunately, since samples of [O III] $\lambda 5007$ selected planetary nebulae are not affected by field contamination, a relatively simple nonparametric test is available to test the null hypothesis, that a set of data is inconsistent with a postulated PNLf. For a given distance modulus, an observationally determined cumulative planetary nebula luminosity function can be compared with a theoretical curve via the Kolmogorov-Smirnov test. The resulting statistic is a good indicator of how well the observations match the theory, and therefore increases the confidence in the maximum-likelihood result.

VII. APPLICATIONS IN THE LOCAL GROUP

The earliest suggestion that PNs may be useful as standard candles originated in the observed constancy of the [O III] luminosity for the brightest PNs in the Local Group galaxies (Ford and Jenner 1978; Jacoby and Lesser 1981). Those assessments, however, were based on photographic and photoelectric measurements in situations where CCD-based observations are far superior. Therefore we have reobserved the central regions of M32, NGC 205, and NGC 185 to derive more accurate photometric measurements of the brightest PNs in these galaxies.

All the galaxies were observed with the Kitt Peak No. 1 0.9 m telescope in its $f/7.5$ configuration using an RCA CCD, which yielded a scale of $0''.86$ pixel $^{-1}$. In addition, M32 was also observed with a TI CCD at the $f/13.5$ focus of the No. 1 0.9 m and with an RCA CCD on the Kitt Peak 2.1 m telescope. The improved spatial scales of $0''.24$ and $0''.38$ pixel $^{-1}$ provided better photometric results for those PNs close to the center of the bright nucleus (see Ford 1983). A summary of the observations is presented in Table 5. A list of the PNs observed and their derived [O III] $\lambda 5007$ magnitudes is given in Table 6. For NGC 185, the planetary nebula identifications are those of

TABLE 5
LOG OF LOCAL GROUP PLANETARY NEBULA OBSERVATIONS

Galaxy	UT Date	KPNO Telescope	CCD	Scale (arcsec pixel $^{-1}$)	Exposure (s)	Filter λ_c /FWHM (Å)
NGC 185	1982 Sep 15	0.9 m	RCA 1	0.86	3600	5009/23
NGC 205	1984 Nov 1	0.9 m	RCA 1	0.86	3600	5004/27
NGC 205	1985 Oct 14	0.9 m	RCA 3	0.86	3600	5004/27
M32	1984 Nov 2	0.9 m	RCA 1	0.86	3600	5004/27
M32	1987 Sep 1	2.1 m	RCA 1	0.38	900	5012/42
M32	1987 Sep 1	2.1 m	RCA 1	0.38	900	5012/42
M32	1987 Oct 7	0.9 m	TI 2	0.24	3600	5004/27

TABLE 6
PLANETARY NEBULAE IN NGC 185, NGC 205, AND M32

Galaxy	PN	$\alpha(1975)$	$\delta(1975)$	m_{5007}	Comment
NGC 185.....	1	0 ^h 37 ^m 33 ^s .62	48°11'08".0	20.34	
	2	0 37 30.02	48 11 54.3	21.40	
	3	0 37 37.10	48 11 39.9	21.68	
	4	0 37 24.90	48 11 18.1	22.78	
	5	0 37 34.17	48 11 56.7	21.54	
NGC 205.....	1	0 38 59.47	41 34 12.7	21.63	
	2	0 39 18.55	41 30 53.0	21.81	
	3	0 39 14.20	41 33 50.0	22.47	
	4	0 38 46.85	41 32 30.8	21.17	
	5	0 38 51.51	41 30 28.6	20.67	
	6	0 38 52.52	41 29 28.5	20.96	
	7	0 38 55.91	41 30 19.4	21.25	
	8	0 38 57.88	41 30 11.1	21.29	
	9	0 38 58.29	41 30 04.1	21.14	
	10	0 39 02.72	41 29 14.4	21.91	
	11	0 39 03.43	41 31 53.2	22.28	
	12	0 38 44.08	41 31 16.9	24.93	
	13	0 38 59.17	41 30 25.3	22.93	
	14	0 39 02.13	41 29 35.6	...	Outside CCD survey
	15	0 39 10.27	41 30 49.6	22.68	
	16	0 38 34.59	41 27 06.0	...	Outside CCD survey
	17	0 39 06.68	41 24 46.8	...	Outside CCD survey
	19	0 38 40.73	41 34 00.7	...	Outside CCD survey
	21	0 39 03.57	41 37 13.3	...	Outside CCD survey
	24	0 38 41.33	41 35 46.6	...	Outside CCD survey
	25	0 38 58.99	41 33 28.6	22.41	
	26	0 39 06.18	41 31 02.9	22.85	
	27	0 38 58.46	41 30 30.5	22.90	
	28	0 38 56.50	41 31 20.4	23.22	
	Star a	0 39 04.17	41 30 33.9	...	
	Star b	0 39 12.57	41 33 54.5	...	
	Star d	0 38 59.10	41 33 59.3	...	
	Star e	0 38 41.22	41 33 58.1	...	
Star f	0 38 54.46	41 36 51.4	...		
Star g	0 38 51.43	41 27 13.1	...		
Star h	0 38 48.71	41 29 34.3	...		
Star j	0 39 01.68	41 30 00.1	...		
Star k	0 39 01.08	41 28 27.4	...		
M32	1	0 41 13.74	40 44 47.6	22.00	
	2	0 41 30.85	40 40 47.1	...	Outside CCD survey
	3	0 41 18.03	40 42 49.4	21.04	
	4	0 41 08.91	40 44 51.9	21.22	Nonmember
	5	0 41 17.43	40 44 27.3	20.93	
	6	0 41 18.18	40 44 30.6	21.31	
	7	0 41 26.00	40 46 00.4	...	Outside CCD survey
	8	0 41 39.88	40 41 18.0	...	Outside CCD survey
	9	0 41 17.92	40 41 28.4	22.05	
	10	0 41 22.81	40 44 35.0	22.83	
	11	0 41 34.78	40 42 48.8	23.28	
	12	0 41 32.37	40 43 54.4	> 23.3	Nonmember
	13	0 41 22.34	40 39 55.2	...	Outside CCD survey
	14	0 41 18.07	40 42 47.1	22.85	
	15	0 41 14.33	40 43 15.4	> 23.3	
	17	0 41 04.82	40 41 28.9	22.15	Nonmember
	18	0 41 09.27	40 45 10.0	23.33	
	19	0 41 14.70	40 41 49.9	> 23.3	
	20	0 41 19.50	40 43 18.2	22.48	
	21	0 41 20.06	40 43 26.1	21.09:	Close to nucleus
	22	0 41 27.68	40 42 57.5	22.65	
	23	0 41 20.07	40 43 36.0	21.61	
	24	0 41 20.36	40 43 43.7	21.50:	Blended with PN 25
	25	0 41 20.52	40 43 43.6	21.37:	Blended with PN 24
	26	0 41 20.05	40 43 48.2	21.39:	Close to nucleus
	27	0 41 19.76	40 43 45.4	20.70:	Close to nucleus
	29	0 41 33.78	40 42 59.7	21.14	
	30	0 41 00.99	40 42 09.6	22.57	

Ford, Jacoby, and Jenner (1977); for NGC 205, the identification numbers include and continue from those given by Ford, Jenner, and Epps (1973) and Ford (1978). The PNs in M32 are from Ford and Jenner (1975) and Ford (1983). Note that three of the planetaries projected in the field of M32 have velocity measurements which place them in M31's background spiral arm, rather than in the elliptical galaxy (Ford and Jenner 1975). To facilitate spectroscopic observations, the positions of astrometric reference stars in the field of NGC 205 are also included in the table.

Table 7 illustrates the constancy of the [O III] $\lambda 5007$ luminosity of the brightest PNs in six local Group galaxies with reasonably well-determined distances. The data for the Magellanic Cloud PNs are derived from the literature, whereas the PN magnitudes for the other galaxies are from the observations described in this paper. From the table, the mean absolute magnitude of the brightest PNs in the galaxies is $M_{5007} = -4.08$, with a standard deviation of 0.15 mag. This dispersion, though comparable to that of other good standard candles, such as the optical period-luminosity relationship of Cepheids (Pel 1985), is actually an upper limit. In addition to the usual uncertainties related to the distances and extinctions toward these galaxies, two other factors affect the luminosities of these brightest PNs.

The first source of dispersion in the Local Group average is the variation in the metallicities of the progenitor stars. Although the [O III] luminosity of a PN will change with metal abundance, Paper I does note that this effect is moderated by a square-root dependence. For example, the Magellanic Cloud PNs (Aller *et al.* 1987) have oxygen abundances which are roughly a factor of 2.5–3 lower than those in M31 (Jacoby and Ford 1986), yet the [O III] luminosities for the brightest LMC and SMC PNs are only 1.33 times smaller than the brightest PN in M31.

A much more important source of scatter in the data of Table 7 comes from the statistics of the PNLF itself. Except for M31, the galaxies listed in Table 7 are all low-luminosity objects, hence the total number of planetaries within each galaxy is small and the number of bright PNs smaller still. For example, the brightest planetary in NGC 205 is over half a magnitude fainter than M^* . Yet if we adopt the distance and extinction listed in Table 7 and the luminosity function given

by equation (2), there is approximately a 30% chance that none of the 13 PNs in the statistically complete sample will have an absolute magnitude brighter than this. A similar condition exists for M32—there is a 25% chance that none of the eight planetaries in the sample with $m_{5007} < 22.7$ will have a luminosity within 0.75 mag of M^* . M31, however, is perhaps the best case study. In the statistically complete sample of 104 planetaries with $m_{5007} < 22.7$, the brightest object is ~ 0.12 mag fainter than M^* . The probability of this happening, however, is almost 60%. A large degree of scatter is therefore expected when comparing planetaries drawn from small sample sizes.

A better way of displaying the statistical uncertainty associated with the PN observations of M32, NGC 205, and NGC 185 is through the PNLF maximum-likelihood analysis. Before such a calculation can be performed, however, three pieces of information must be known.

As explained in § VI, the completeness limit is crucial for any maximum-likelihood analysis, since this value provides the normalization for the equations. When large numbers of objects are involved, histograms of number versus magnitude provide a useful tool for understanding the observational limits. However, when the number of objects is small, this limiting magnitude can sometimes be difficult to calculate. Fortunately, in the present case, the observing conditions and exposure times for M32 and NGC 205 were similar to those for M31. Hence M31's PN boundary conditions can be applied: when the surface brightness of the background galaxy is less than $m_r = 17.5$, a conservative upper limit for completeness is $m_{5007} = 22.7$; when the background galaxy is as bright as $m_r = 16.2$, the completeness limit is closer to $m_{5007} = 22.0$. While the former condition is appropriate for virtually all of NGC 205, NGC 185, and the areas of M32 more than $18''$ away from its nucleus, the latter limit allows planetaries as close as $7''$ from M32's nucleus to be included.

The second quantity needed for the maximum-likelihood analysis is the integrated bolometric galaxy magnitude contained in the PN survey fields. In order to calculate this, the surface photometry and transformations of Kent (1987) were used to estimate the total V luminosity encompassed in the survey areas. Bolometric corrections appropriate for each galaxy were then computed from the $(B - V)$ colors of Penston

TABLE 7
BRIGHTEST PLANETARY NEBULAE IN LOCAL GROUP GALAXIES

Galaxy	PN Identification	$\log F(\lambda 5007)$ ($\text{ergs cm}^{-2} \text{s}^{-1}$)	$E(B - V)$	Distance (kpc)	M_{5007}	Distance Reference
M31	380	-13.61	0.11	710	-4.36	Pritchett and van den Bergh 1987; Welch <i>et al.</i> 1986
LMC	P25	-11.30	0.03	50	-4.09	Schommer, Olszewski, and Aaronson 1984; Torres, Conti, and Massey 1986
SMC	N2	-11.70	0.20	60	-4.10	Da Costa and Mould 1986; Mathewson, Ford, and Visvanathan 1986; Garmany, Conti, and Massey 1987
M32	27	-13.78	0.11	710	-3.94	Assumed equal to M31
NGC 205	5	-13.76	0.06	760	-3.95	Richer, Crabtree, and Pritchett 1984; Mould, Kristian, and Da Costa 1984
NGC 185	1	-13.63	0.17	570	-4.04	Saha and Hoessel 1988

NOTES.—M31—PN identification (ID) and photometry from this paper. LMC—PN ID from Westerlund and Smith 1964; photometry from Webster 1969. SMC—PN ID from Henize 1956; photometry from Osmer 1976. M32—PN ID from Ford 1983; photometry from this paper. NGC 205—PN ID from Ford, Jenner, and Epps 1973; photometry from this paper. NGC 185—PN ID from Ford, Jacoby, and Jenner 1977; photometry from this paper.

(1973), Price and Grasdalen (1983), and Price (1985), and the infrared colors of Frogel *et al.* (1978). The total luminosity sampled in each galaxy, along with the bolometric corrections, and nominal luminosity-specific densities for planetaries in the top 2.5 mag of the PNLF appear in Table 8.

The last piece of information required by the discussion in § VI is some knowledge of the photometric measurement error versus magnitude. Although, strictly speaking, these errors are a function of both the object's flux and the background surface brightness, in practice the latter contribution dominates only where the background galaxy is brightest and incompleteness is a problem anyway. The problem is therefore tractable, though not always easily solved. Fortunately, in this specific case, the M31 observations could again be used to simplify the task. The 232 M31 planetaries with multiple measurements and isophotal radii $r_{\text{iso}} > 15''$ were binned into 0.25 mag intervals and the within-class magnitude variance calculated for each bin. A smooth curve was then fitted through the data defining the expected standard error versus magnitude. This error begins at 0.03 mag at $m_{5007} = 20.4$, slowly increases to 0.10 mag at $m_{5007} = 22.0$, and then rises rapidly to 0.18 mag at $m_{5007} = 22.7$.

Figures 6a–6d display the confidence level contours in (μ, α) -space implied by the distribution of planetary nebula [O III] luminosities observed in M31, M32, NGC 205, and NGC 185. Note that the contours deviate from circularity in the sense that the distance modulus may be smaller if α is allowed to assume larger values. Physically, this means that confusion arises between a distant luminous galaxy having a small population of planetaries, and a nearby low-luminosity galaxy with a large PN population. This effect is dramatically demonstrated for the three small ellipticals in Figures 6b–6d.

The distance modulus to M31 is very tightly constrained, even at the 3σ level, to $23.80 < \mu_0 < 24.40$; the luminosity-

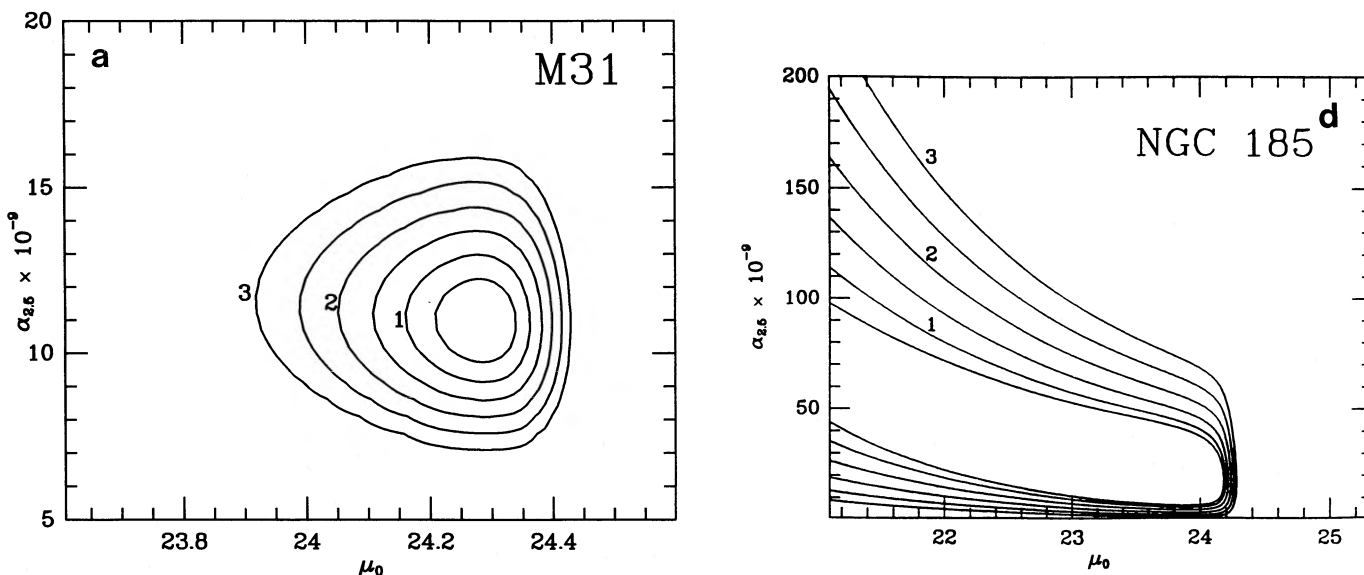


FIG. 6.—(a) Maximum-likelihood confidence contours for M31 derived from a complete sample of 104 PNs and assuming the empirical PNLF expressed in eq. (2). The abscissa is the true distance modulus, μ_0 ; the ordinate is the number of planetaries within 2.5 mag of M^* normalized to the absolute bolometric luminosity of the survey region. The curves labeled 1, 2, and 3 refer to multiples of σ , where 1σ , 2σ , and 3σ correspond to confidence intervals of 68%, 95%, and 99.7%, respectively. Intermediate contours of 0.5σ , 1.5σ , and 2.5σ are also shown. The solution has been constrained to yield a most probable distance modulus of 24.25, but the dispersion is representative of what can be expected from PNLF fitting. (b–d) Confidence contours for M31's companion galaxies, M32, NGC 205, and NGC 185. The abscissa is the true distance modulus, μ_0 ; the ordinate is the number of planetaries within 2.5 mag of M^* normalized to the absolute bolometric luminosity of the galaxy. For purposes of this presentation, the diagrams have been enlarged so that some contours close outside the displayed area. Probabilities are based on eight, 13, and four PNs for the three galaxies, respectively. Inspection of (b) and (c) suggests that M32 and NGC 205 are at nearly identical distances, while (d) demonstrates that NGC 185 is very likely closer.

TABLE 8
LUMINOSITY-SPECIFIC DENSITIES FOR PLANETARY NEBULAE WITHIN 2.5 MAGNITUDES OF M^*

Galaxy	$(M^* - M)$	Number of PNs	m_V	BC	M_{bol}	PN/ $(L_{\text{bol}})_{\odot}$ ($\times 10^{-9}$)
NGC 185	2.5	4	9.65	-0.60	-15.39	39.4
NGC 205	2.5	12	8.84	-0.45	-16.20	50.1
M32	1.5	9	8.39	-0.80	-17.01	33.7
M32	2.5	8	8.64	-0.80	-16.75	22.3

specific number density of PN is restricted to values between 8×10^{-9} and 18×10^{-9} , although again, owing to the presence of dust, the latter quantity may be underestimated. Since we defined the zero point of the PNLF using M31, the derived value for the most probable distance contains no new information. The dispersion in allowable distances is not entirely independent either, since the form of the PNLF used in the maximum-likelihood procedure was, in part, based on M31 observations. Future papers in this series will present additional data from other well-observed galaxies to support the adopted PNLF, and therefore strengthen the usefulness of the M31 distance limits derived here.

For M32 and NGC 205 (Figs. 6b and 6c), the most probable distances are in good agreement with the values in Table 7, but the error contours occupy considerable area in the (μ, α) -plane. In the case of NGC 205, the "best-fit" value for the specific PN number density is almost a factor of 3 higher than that seen in M31, but values as low as M31's are not excluded. A Kolmogorov-Smirnov test comparing the observed PNLF of

each galaxy with the theoretical PNLF also shows agreement, with the null hypothesis being rejected at the 99% confidence level. Because of the small sample of planetaries in each galaxy, however, this is not a powerful result.

Because of the very small sample (4) of PN in NGC 185, the probability contours for this galaxy are essentially unconstrained with one important exception. For any galaxy with identified PN, there exists a sharp upper limit to the derived distance. This results naturally from the hard upper limit to the allowable luminosity for all planetaries. We see that the distance modulus for NGC 185 is therefore strongly bounded to be less than 24.3 at the 3σ confidence level. Similar limits can be seen for the other three galaxies in the figure.

We wish to thank Morton Roberts for the Palomar Schmidt plate reproduced in Figure 1. Thanks also go to Nigel Sharp for some helpful insights into the utility of probability contours.

REFERENCES

- Aller, L. H., Keyes, C. D., Maran, S. P., Gull, T. R., Michalitsianos, A. G., and Stecher, T. P. 1987, *Ap. J.*, **320**, 159.
 Baade, W. 1955, *A.J.*, **60**, 151.
 Ciardullo, R., Ford, H. C., Neill, J. D., Jacoby, G. H., and Shafter, A. W. 1987, *Ap. J.*, **318**, 520.
 Ciardullo, R., Jacoby, G. H., and Ford, H. C. 1989, in preparation.
 Ciardullo, R., Rubin, V. C., Jacoby, G. H., Ford, H. C., and Ford, W. K., Jr. 1988, *A.J.*, **95**, 438.
 Coleman, G. D., Wu, C.-C., and Weedman, D. W. 1980, *Ap. J. Suppl.*, **43**, 393.
 Da Costa, G. S., and Mould, J. R. 1986, *Ap. J.*, **305**, 214.
 de Vaucouleurs, G., and Pence, W. D. 1978, *A.J.*, **83**, 1163.
 Drilling, J. S., and Schönberner, D. 1983, in *IAU Symposium 105, Observational Tests of the Stellar Evolution Theory*, ed. A. Maeder and A. Renzini (Dordrecht: Reidel), p. 219.
 Eddington, A. S. 1913, *M.N.R.A.S.*, **73**, 359.
 Ford, H. C. 1978, in *IAU Symposium 76, Planetary Nebulae*, ed. Y. Terzian (Dordrecht: Reidel), p. 19.
 ———. 1983, in *IAU Symposium 103, Planetary Nebulae*, ed. D. R. Flower (Dordrecht: Reidel), p. 443.
 Ford, H. C., Ciardullo, R., Jacoby, G. H., and Hui, X. 1988, in *IAU Symposium 131, Planetary Nebulae*, ed. S. Torres-Peimbert (Dordrecht: Reidel), in press.
 Ford, H. C., and Jacoby, G. H. 1978a, *Ap. J.*, **219**, 437.
 ———. 1978b, *Ap. J. Suppl.*, **38**, 351.
 Ford, H. C., Jacoby, G., and Jenner, D. C. 1977, *Ap. J.*, **213**, 18.
 Ford, H. C., and Jenner, D. C. 1975, *Ap. J.*, **202**, 365.
 ———. 1978, *Bull. AAS*, **10**, 665.
 Ford, H. C., Jenner, D. C., and Epps, H. W. 1973, *Ap. J. (Letters)*, **183**, L73.
 Frogel, J. A., Persson, S. E., Aaronson, M., and Matthews, K. 1978, *Ap. J.*, **220**, 75.
 Gallagher, J. S., and Hunter, D. A. 1981, *A.J.*, **86**, 1312.
 Garmany, C. D., Conti, P. S., and Massey, P. 1987, *A.J.*, **93**, 1070.
 Hanes, D. A., and Whittaker, D. G. 1987, *A.J.*, **94**, 906.
 Heber, U., Hunger, K., Kudritzki, R. P., and Simon, K. P. 1983, in *IAU Symposium 105, Observational Tests of Stellar Evolution Theory*, ed. A. Maeder and A. Renzini (Dordrecht: Reidel), p. 215.
 Henize, K. G. 1956, *Ap. J. Suppl.*, **2**, 315.
 Henize, K. G., and Westerlund, B. E. 1963, *Ap. J.*, **137**, 747.
 Hodge, P. W. 1966, *The Physics and Astronomy of Galaxies and Cosmology* (New York: McGraw-Hill), p. 130.
 ———. 1980, *A.J.*, **85**, 376.
 Jacoby, G. H. 1980, *Ap. J. Suppl.*, **42**, 1.
 ———. 1989, *Ap. J.*, **339**, 39 (Paper I).
 Jacoby, G. H., and Ford, H. C. 1986, *Ap. J.*, **304**, 490.
 Jacoby, G. H., Hunter, D. A., and Christian, C. A. 1984, *Ap. J. Suppl.*, **56**, 257.
 Jacoby, G. H., and Lesser, M. P. 1981, *A.J.*, **86**, 185.
 Jacoby, G. H., Quigley, R. J., and Africano, J. L. 1987, *Pub. A.S.P.*, **99**, 672.
 Johnson, H. L. 1966, *Ann. Rev. Astr. Ap.*, **4**, 193.
 Johnson, H. M., and Hanna, M. M. 1972, *Ap. J. (Letters)*, **174**, L71.
 Kent, S. M. 1983, *Ap. J.*, **266**, 562.
 ———. 1987, *A.J.*, **94**, 306.
 Kudritzki, R. P., Mendez, R. H., and Simon, K. P. 1983, in *IAU Symposium 205, Observational Tests of the Stellar Evolution Theory*, ed. A. Maeder and A. Renzini (Dordrecht: Reidel), p. 205.
 Lawrie, D. G., and Ford, H. C. 1982, *Ap. J.*, **256**, 120.
 Lawrie, D. G., and Graham, J. A. 1983, *Bull. AAS*, **15**, 907.
 Mathewson, D. S., Ford, V. L., and Visvanathan, N. 1986, *Ap. J.*, **301**, 664.
 McClure, R. D., and Racine, R. 1969, *A.J.*, **74**, 1000.
 McElroy, D. B. 1983, *Ap. J.*, **270**, 485.
 Mould, J., and Kristian, J. 1986, *Ap. J.*, **305**, 591.
 Mould, J., Kristian, J., and Da Costa, G. S. 1984, *Ap. J.*, **278**, 575.
 Nolthenius, R., and Ford, H. C. 1987, *Ap. J.*, **317**, 62.
 Oke, J. B. 1974, *Ap. J. Suppl.*, **27**, 21.
 Osmer, P. S. 1976, *Ap. J.*, **203**, 352.
 Pell, J. W. 1985, in *Cepheids: Theory and Observations*, ed. B. F. Madore (Cambridge: Cambridge University Press), p. 1.
 Penston, M. V. 1973, *M.N.R.A.S.*, **162**, 359.
 Pottasch, S. R. 1984, *Planetary Nebulae: A Study of Late Stages of Stellar Evolution* (Dordrecht: Reidel), p. 215.
 Price, J. S. 1985, *Ap. J.*, **297**, 652.
 Price, J. S., and Grasdalen, G. L. 1983, *Ap. J.*, **275**, 559.
 Pritchett, C. J., and van den Bergh, S. 1987, *Ap. J.*, **316**, 517.
 Renzini, A., and Buzzoni, A. 1986, in *Spectral Evolution of Galaxies*, ed. C. Chiosi and A. Renzini (Dordrecht: Reidel), p. 195.
 Richer, H. B., Crabtree, D. R., and Pritchett, C. J. 1984, *Ap. J.*, **287**, 138.

- Saha, A., and Hoessel, J. G. 1988, private communication.
Sandage, A. R., Becklin, E. E., and Neugebauer, G. 1969, *Ap. J.*, **157**, 55.
Schönberner, D. 1983, *Ap. J.*, **272**, 708.
Schommer, R. A., Olszewski, E. W., and Aaronson, M. 1984, *Ap. J. (Letters)*, **285**, L53.
Seaton, M. J. 1979, *M.N.R.A.S.*, **187**, 73P.
Stone, R. P. S. 1977, *Ap. J.*, **218**, 767.
Torres, A. V., Conti, P. S., and Massey, P. 1986, *Ap. J.*, **300**, 379.
Webster, B. L. 1969, *M.N.R.A.S.*, **143**, 79.
Welch, D. L., McAlary, C. W., McLaren, R. A., and Madore, B. F. 1986, *Ap. J.*, **305**, 583.
Westerlund, B. E., and Smith, L. F. 1964, *M.N.R.A.S.*, **127**, 449.
Wu, C.-C., et al. 1983, *IUE Ultraviolet Spectral Atlas (IUE NASA Newsletter)* No. 22).

ROBIN CIARDULLO and GEORGE H. JACOBY: Kitt Peak National Observatory, P.O. Box 26732, Tucson, AZ 85726

HOLLAND C. FORD and JAMES D. NEILL: Space Telescope Science Institute, 3700 San Martin Drive, Baltimore, MD 21218